IMPLEMENTATION OF A CALIBRATION PROCEDURE FOR A SIX-PORT MICROWAVE MEASUREMENT SYSTEM

BY

JOHN CHARLES WOODS

A Thesis
submitted to the Faculty of Graduate Studies
of the University of Manitoba
in partial fulfillment of the
requirements of the degree of

MASTER OF SCIENCE

Department of Electrical Engineering

IMPLEMENTATION OF A CALIBRATION PROCEDURE FOR A SIX-PORT MICROWAVE MEASUREMENT SYSTEM

BY

JOHN CHARLES WOODS

A thesis submitted to the Faculty of Graduate Studies of the University of Manitoba in partial fulfillment of the requirements of the degree of

MASTER OF SCIENCE

ACKNOWLEDGEMENTS

The author would like to thank professor E. Bridges for his continual support and guidance in all phases of this work. Thanks are also due to Mr. B. Tabachinick for his help and support.

ABSTRACT

In this thesis an automated six-port microwave measurement system is developed and tested to measure the complex reflection coefficient of microwave devices. A six-port network consisting of a five-way symmetric power divider and a 90 hybrid is the heart of the system.

The six-port is calibrated using a matched load, four short circuited lines and a new calibration procedure which minimizes errors due to system imperfections. This procedure also allows the use of the same calibration shorts for the entire bandwidth of the instrument. In the past, different shorts were needed for each frequency. Four simple diode detectors are used to measure the power at four ports of the network and from these the reflection coefficient is determined.

The temperature (and electrical characteristics) of the detectors was stabilized using a temperature controlled oven. Details of this oven are given in this thesis. The detectors were characterized using a fourth order polynomial relating the incident microwave power to the output dc voltage.

The system was tested over a 200 MHz bandwidth centered at 1 GHz. Results show good agreement (within a few percent) for most of the band of interest. Deviations of up to 15 percent were found at the upper band edge.

Chapter I

INTRODUCTION

Reflection coefficient measurements have been performed for many years with instruments such as the slotted line, directional coupler, microwave bridge and the automatic network analyzer (ANA). In 1977 the complex reflection coefficient was first measured using a network device known as the six-port reflectometer [1]. This thesis describes the development and testing of an automated six-port reflectometer system. The system is made up of a five-way symmetrical power divider, a 90 degree hybrid junction and four diode amplitude detectors ; with control and data acquisition provided by an HP 85 desktop computer.

Chapter I of this thesis is devoted to necessary six-port network theory and a description of a few previously reported systems. The six-port reflectometer determines the reflection coefficient of a terminating device by measuring the power at four ports of the network. The reflection coefficient is calculated from these power readings using equations derived from six-port theory [2] and seven pre-determined calibration constants. Chapter II introduces background six-port theory and presents a new procedure [3] for determining the calibration constants which minimizes

errors due to system imperfections. In this procedure a matched load and four short circuited coaxial lines are used to calibrate the six-port system at any frequency within a specified frequency band. This new procedure allows the same set of reference shorted lines to be used to determine the calibration constants at any frequency in the band. Previous procedures needed four lines, each of specific length, for each calibration frequency.

The actual six-port system and its components are described in Chapter III. The software for both calibration and determination of reflection coefficient are also found in Chapter III.

The electrical characteristics of the diode detectors used to measure RF power change significantly with temperature and are a major source of errors. For this reason a temperature controlled oven was designed and built to house the detectors and stabilize each detector's temperature to within $\pm$ 0.5 $^{\circ}$C. Each detector was characterized by measuring the detector's output dc voltage as a function of input RF power for a prescribed range of power levels. This voltage versus power data was applied to a curve fitting procedure to determine the coefficients of a fourth order polynomial which relates the voltage to the input power. The RF power incident on a detector could then be closely estimated by measuring the dc voltage at the detector output and applying the polynomial approximation.

Chapter IV of this paper deals with the details of the detector power calibration.

Chapter V presents results of experimentation with the reflectometer system. First the calibration constants were determined for the frequency band of interest, 200 MHz centered at 1 GHz, in 50 MHz steps. These results are compared to ideal calibration constants and to constants found for the same six-port network by another investigator [11] using a different calibration procedure, with good results. Secondly, the system was used to measure the reflection coefficient of several loads at different frequencies. These measurements were compared to those made with an ANA and a slotted line with agreement to within a few percent for most of the frequency band.

Chapter VI presents conclusions and includes some general comments on the use of the automated six-port system.

The rest of this chapter is devoted to necessary six-port network theory and a description of a few previously reported systems.

1.1 PREVIOUS SIX PORTS

In 1972 Hoer and Engen [2] published their work on a six port measurement system which made use of simple amplitude detectors and several directional couplers to measure the power incident on a load. An equation is derived from the scattering parameters of an arbitrary six-port junction which relates the net power at the test port to the power measured at the other ports.

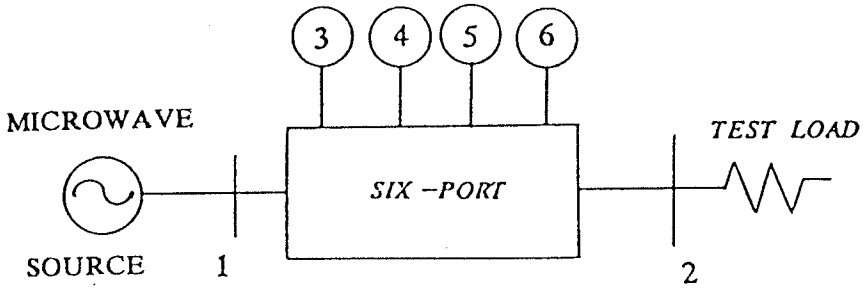

Figure 1.1: AN ARBITRARY SIX-PORT NETWORK

For the system shown in figure 1.1 we can write

$$b_i = \sum_{j=1}^{6} S_{ij} a_j \qquad i = 1 \cdots 6 \tag{1.1}$$

and at ports 3 to 6

$$a_j = b_j \Gamma_j \qquad j = 3 \cdots 6 \tag{1.2}$$

where Γ_j is the reflection coefficient of the power meter terminating port j and is considered fixed. The a_i and b_i are the complex amplitudes of the incoming and outgoing waves at port i. These ten linear relationships of twelve terminal variables can be used to solve for any ten variables in terms of the remaining two. For instance :

$$b_i = r_i a_2 + t_i b_2 \qquad i = 3 \cdots 6 \tag{1.3}$$

where r_i and t_i are functions of Γ_j and $[S]$, the scattering parameters of the network. We can write the power at port i as

$$P_i = |b_i|^2 = |r_i|^2|a_2|^2 + r_i t_i^* a_2 b_2^* + r_i^* t_i a_2^* b_2 + |t_i|^2|b_2|^2 \qquad i = 3 \cdots 6 . \tag{1.4}$$

Now $|a_2|$ and $|b_2|$ could be solved for in terms of $P_i (i = 3 \cdots 6)$ and

$$P_{2net} = |b_2|^2 - |a_2|^2 = \sum_{i=3}^{6} q_i P_i \tag{1.5}$$

where q_i are functions of $[S]$ and Γ_j only and are the six-port constants to be determined. To find the q_i, port 2 is first terminated with a power meter so that P_2 is known and $P_i \quad i = 3 \cdots 6$ are measured. Now the power meter is replaced by three offset shorts with $P_2 = 0$. P_i are again

measured and equation (1.5) is inverted and used to determine q_i . The actual system tested in [2] is shown in figure 1.2.

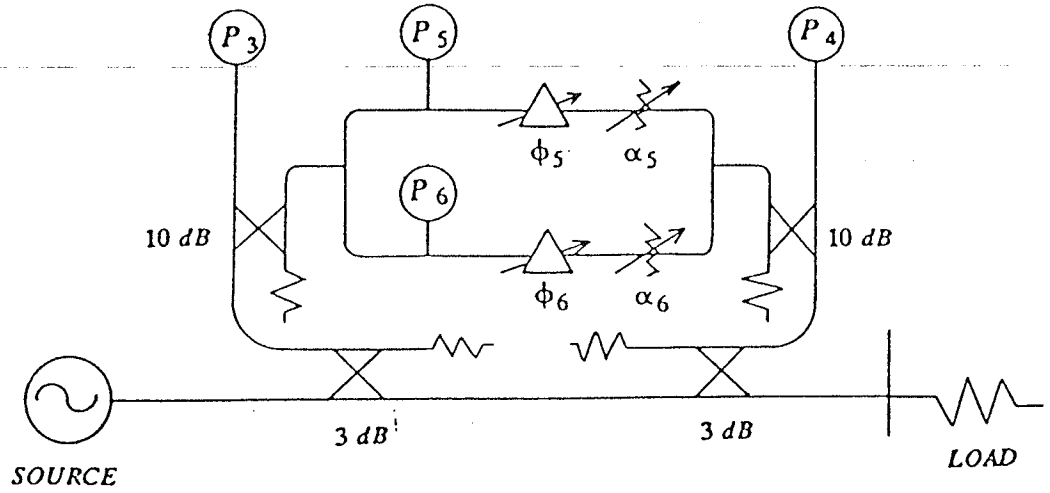

Figure 1.2: AN EARLY SIX-PORT NETWORK

where all the components are X band waveguide. This system agreed well with generalized reflectometer measurements to better than 0.25 % when measuring power incident at port 2.

The magnitude of the reflection coefficient for a load at port 2 can be found by taking the ratio of b_3 to b_4 . But to measure the phase, frequency conversion is necessary adding expense and complexity to the system. Modern day automatic network analyzers (ANA) use frequency conversion and are indeed very complex.

Engen continued work on the six-port and in 1977 developed a system , [1] and [4], (using three quadrature couplers and a hybrid) which measured both magnitude and

phase of the reflection coefficient of a terminating device. Four simple amplitude detectors were again used. Figure 1.3 shows the system.

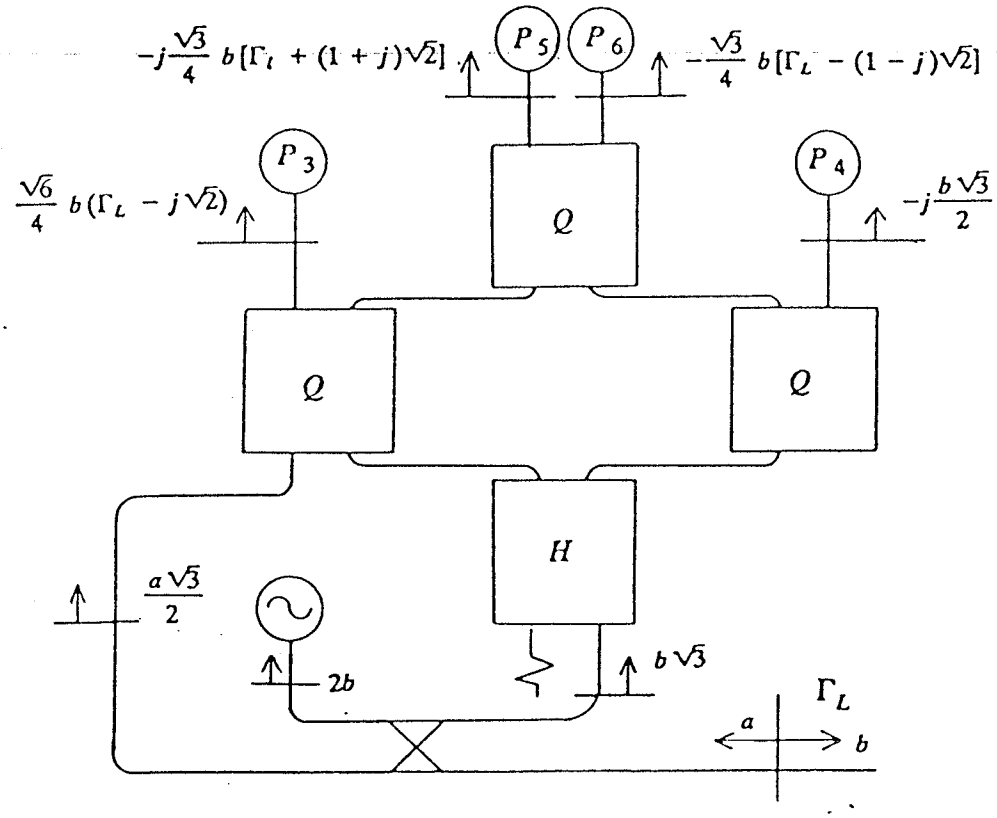

Figure 1.3: A PROPOSED SIX PORT

In general for the power measured at the four detectors we can write

$$P_3 = |b_3|^2 = |A\,a_2 + B\,b_2|^2 , \tag{1.6a}$$

$$P_4 = |C\,a_2 + D\,b_2|^2 , \tag{1.6b}$$

$$P_5 = |E\,a_2 + F\,b_2|^2 , \tag{1.6c}$$

$$P_6 = |G\,a_2 + H\,b_2|^2 , \tag{1.6d}$$

where A ... H are complex constants determined by the system. Equations (1.6a) ... (1.6d) can be rewritten as

$$P_3 = |A|^2 |b_2|^2 |\Gamma_L - q_3|^2 , \tag{1.7a}$$

$$P_5 = |E|^2 |b_2|^2 |\Gamma_L - q_5|^2 , \tag{1.7b}$$

$$P_6 = |G|^2 |b_2|^2 |\Gamma_L - q_6|^2 , \tag{1.7c}$$

where $q_3 = -\frac{B}{A}$, $q_5 = -\frac{F}{G}$, $q_6 = -\frac{H}{G}$ and $\Gamma_L = a_2 / b_2$.

If we can design the system such that C=0 (which is nearly possible for a good directional coupler incorporated in the six-port and well matched detectors), and consider P_4 to be a reference power, then

$$|b_2|^2 = P_4 / |D|^2 . \tag{1.8}$$

We can eliminate $|b_2|^2$ in (1.7) with the result

$$|\Gamma_L - q_3|^2 = |\frac{D}{A}|^2 \frac{P_3}{P_4} ,$$

$$|\Gamma_L - q_5|^2 = |\frac{D}{E}|^2 \frac{P_5}{P_4} , \tag{1.9}$$

$$|\Gamma_L - q_6|^2 = |\frac{D}{G}|^2 \frac{P_6}{P_4} .$$

If $q_3, q_5, q_6, P_3, P_4, P_5, P_6, |D/A|^2, |D/E|^2$ and $|D/G|^2$ are known we can represent these equations as three circles centered at q_3, q_5, q_6 (known as the q points) on the complex Γ_L plane.

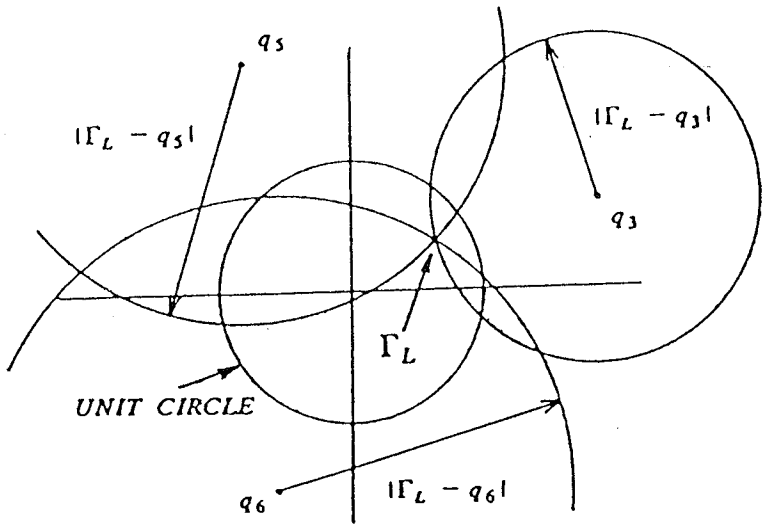

Figure 1.4: Q POINT DISTRIBUTION

The intersection of these circles within the unit circle determines the value of Γ_L in both magnitude and phase. The constants $|A|, |D|, |E|$ and $|G|$ are evidently, from equation (1.9), scale factors which determine the power levels at the four power meters for a given load. These are chosen so that the power levels are compatible with the power meters. Details of the determination of q_3, q_5 and q_6 for the system of figure 1.3 were not disclosed. However, the optimum design criteria were given in [4] as 1) $|q_3| = |q_5| = |q_6| = |q|$, 2) their arguments differ by 120° and 3) the $|q|$ lie in the

range of 0.5 to 1.5. The six port of figure 1.3 only approximately fulfilled these criteria and six-port reflectometer work was continued by Riblet and Hansson [5], [6], Cullen et al [7], Cronson and Susman [8], D. Woods [8] and others. The six-port developed by Riblet and Hansson is of particular interest because it achieved the ideal q point distribution given by Engen [4] using a matched reciprocal lossless five-port power divider similar to the one used in

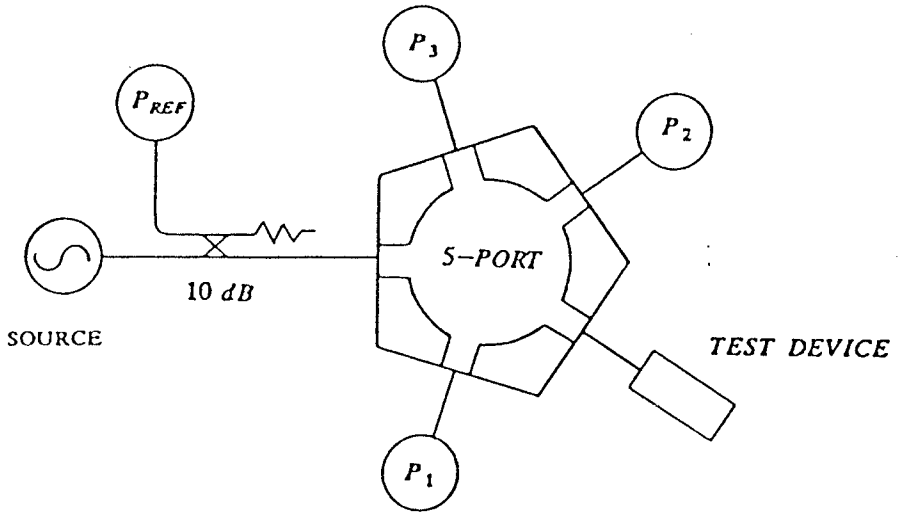

Figure 1.5: RIBLET'S SIX-PORT

this thesis. Riblet's system is shown in figure 1.5. The detector on the directional coupler monitors the power input to the five-port and is known as the reference detector. The scattering matrix for a symmetrical reciprocal five-port has been proven (by Dicke [10]) to have the scattering coefficients given by

$$S_{11} = (S_1 + 2S_2 + 2S_3) / 5 \quad , \tag{1.10}$$

$$S_{12} = S_{15} = [S_1 + 2s_2\cos(2\frac{\pi}{5}) + 2S_3\cos(4\frac{\pi}{5})] / 5 \quad , \tag{1.11}$$

$$S_{13} = S_{14} = [S_1 + 2S_2\cos(4\frac{\pi}{5}) + 2S_3\cos(2\frac{\pi}{5})] / 5 \tag{1.12}$$

where S_1, S_2 and S_3 are eigenvalues which represent the reflection coefficients of three eigen-excitations of the junction. Because the device is assumed lossless, these eigenvalues must have unit amplitude. If we arbitrarily choose the phase of S_1 to be 180° we have

$$\begin{aligned} S_1 &= -1 \quad , \\ S_2 &= e^{j\phi_2} \quad , \\ S_3 &= e^{j\phi_3} \quad . \end{aligned} \tag{1.13}$$

Also if we assume a matched junction condition we have from (1.10)

$$S_{11} = (S_1 + 2S_2 + 2S_3) / 5 = 0$$

and upon substitution of (1.13) that

$$e^{j\phi_2} + e^{j\phi_3} = 1 / 2$$

or

$$\cos\phi_2 + j\sin\phi_2 + \cos\phi_3 + j\sin\phi_3 = 1 / 2 \tag{1.14}$$

Inspection of (1.14) shows that $\phi_2 = \pm\ 75.5^{\circ}$ since $\sin\phi_2 = -\sin\phi_3$ and $\cos\phi_2 = 1 / 4$. Substitution of ϕ_2 and ϕ_3 into (1.11) and (1.12) yields

$$|S_{12}| = |S_{13}| = 1/2 \ ,$$

$$\angle S_{13} = \angle S_{12} = \pm 120^{\circ} .$$

This shows that the five-port acts as a four way equal power divider.

Riblet and Hansson [5] built two five-port ring structures using RT duroid stripline with measured scattering parameters close to theoretical values. In 1983 a six-port device was developed by Jagdish Girimaji [11]. This system was based on Riblet and Hansson's and figure 1.5 can be referred to as the system diagram for his system.

The six-port theory related to Girimaji's system follows very closely with that used by Engen and Hoer [2] which will be described in greater detail in the following chapter. What is important at this stage is Girimaji's calibration procedure since it is essentially different from the one presented later in this thesis. In the next chapter it will be shown that the basic equations governing the six-port system can be generalized as

$$\frac{P_i}{P_R} = |B_i|^2 \frac{X_i^2 |\Gamma_L|^2 + 1 + 2 X_i |\Gamma_L| \cos(\phi_{ix} + \phi_L)}{Z^2 |\Gamma_L|^2 + 1 + 2 Z |\Gamma_L| \cos(\phi_L + \phi_Z)} \qquad (1.15)$$

where P_i is the power measured at detector i = 1,2,3, P_R is the reference incident power; $|B_i|$, X_i , ϕ_{xi} , Z and ϕ_Z are

the calibration constants to be determined. $|\Gamma_L|$ and ϕ_L are the reflection coefficient magnitude and phase, respectively, of a given load at the test port. If a matched load is applied at the test port then $\Gamma_L = 0$ and we see that $|B_i|$ is easily determined from P_i . The remaining constants are found from the measured powers by applying four loads whose reflection coefficient are of known phase and unit magnitude. D. Woods [9] presented a solution whereby the shorts must have specific values to avoid numerical singularities. This is an important difference in the method described in this thesis, where the loads are of unit magnitude but of arbitrary (but known) electrical length.

To calibrate the six-port according to Girimaji's [11] procedure we apply a matched load (to determine the $|B_i|$ as described before) and four shorts of known phase and unit magnitude. He chose $\Gamma_L = 1, -1, \mathrm{j}, \text{and } -\mathrm{j}$ as the calibration standards. The test loads are applied one at a time and four power measurements are made for each load. To determine Z and ϕ_Z we first normalize the measured powers with respect to the reference powers and $|B_i|$ which have been previously determined by the matched load termination, thus

$$R_{ij} = \frac{P_i}{P_R \ |B_i|^2} \quad . \tag{1.16}$$

Writing (1.15) in matrix form and using the normalization of (1.16) we have

$$\begin{bmatrix} R_{1i} & R_{1i}\cos\phi_1 & -R_{1i}\sin\phi_1 \\ R_{2i} & R_{2i}\cos\phi_2 & -R_{2i}\sin\phi_2 \\ R_{3i} & R_{3i}\cos\phi_3 & -R_{3i}\sin\phi_3 \end{bmatrix} \begin{bmatrix} 1+Z^2 \\ 2Z\cos\phi_z \\ 2Z\sin\phi_z \end{bmatrix} = \begin{bmatrix} 1 & \cos\phi_1 & -\sin\phi_1 \\ 1 & \cos\phi_2 & -\sin\phi_2 \\ 1 & \cos\phi_3 & -\sin\phi_3 \end{bmatrix} \begin{bmatrix} 1+X_i^2 \\ 2X_i\cos\phi_{ix} \\ 2X_i\sin\phi_{ix} \end{bmatrix}$$

and
$$R_{0i}(1+Z^2) + R_{0i}\cos\phi_0\, 2Z\cos\phi_Z - R_{0i}\sin\phi_0\, 2Z\sin\phi_Z = 1 + X_i^2 + \cos\phi_0\, 2X_i\cos\phi_{xi} - \sin\phi_0\, 2X_i\sin\phi_{xi} \quad . \tag{1.17}$$

The solution of this matrix equation (see appendix A) gives

$$\begin{aligned} A_{11}\left(Z + \frac{1}{Z}\right)/2 + A_{12}\cos\phi_Z + A_{13}\sin\phi_Z &= 0 \quad , \\ A_{21}\left(Z + \frac{1}{Z}\right)/2 + A_{22}\cos\phi_Z + A_{23}\sin\phi_Z &= 0 \quad , \\ A_{31}\left(Z + \frac{1}{Z}\right)/2 + A_{32}\cos\phi_Z + A_{33}\sin\phi_Z &= 0 \quad . \end{aligned} \tag{1.18}$$

The first two equations when subtracted yield

$$\phi_Z = TAN^{-1}\left[\frac{A_{21}A_{12} - A_{11}A_{22}}{A_{11}A_{23} - A_{21}A_{13}}\right] \quad . \tag{1.19}$$

Once ϕ_Z has been determined we can find Z from

$$A_{11}(1+Z^2) + A_{12}(2Z\cos\phi_Z) + A_{13}(2Z\sin\phi_Z) = 0$$

and

$$1 + Z^2 + 2Z\left(\frac{A_{12}\cos\phi_Z + A_{13}\sin\phi_Z}{A_{11}}\right) = 0 \quad .$$

When these equations are rewritten as

$$Y = -\left(\frac{A_{12}\cos\phi_z + A_{13}\sin\phi_z}{A_{11}}\right) \quad ,$$

$$1 - 2ZY + Z^2 = 0$$

they can be solved by use of the quadratic equation. The ambiguity in $Y \pm \sqrt{Y^2 - 1}$ is overcome since for a passive device, $Z < 1$ (see [11]).

Now the powers at the four ports are measured for each of four shorted lines of known electrical length terminating the test port. These powers and the previously determined Z and ϕ_Z are applied to (1.15) to determine the remaining constants.

The described system and calibration procedure were found to work very well with measured accuracies approaching those using an ANA. The main problem is that the reflection standards must be near exact to specified values and a new set of standards is needed at each calibration frequency.

Chapter II

SIX-PORT CALIBRATION THEORY

The first part of this chapter is devoted to the derivation of the basic equation which relates the six-port constants to the power readings and the reflection coefficient of a device terminating the test port. This equation is then used to obtain equations for the calibration constants in the new calibration procedure. Finally, the basic equation is cast in a form for evaluation of the load reflection coefficient from simple power readings.

2.1 GENERAL SIX-PORT EQUATION

As previously stated, [1], the relationship between the response at a given detector port i and the load at port 2 of a four arm junction is $b_i = r_i\, a_2 + t_i\, b_2$. We can extend this relationship to a six-port [4] and write the response at port 3 and reference port 4 as

$$b_3 = Aa_2 + Bb_2 \ , \tag{2.1}$$

$$b_4 = Ca_2 + Db_2 \tag{2.2}$$

where A,B,C and D are complex constants. If we divide equation (2.1) by (2.2) and use $\Gamma_L = a_2 / b_2$ we have

$$\frac{b_3}{b_4} = \frac{Aa_2 + Bb_2}{Ca_2 + Db_2} = B \frac{(\frac{A}{B}\Gamma_L + 1)}{C\Gamma_L + D} \quad . \tag{2.3}$$

With appropriate scaling (see [7]) we can assume D = 1, so that

$$\frac{b_3}{b_4} = B \frac{(\frac{A}{B}\Gamma_L + 1)}{C\Gamma_L + 1} \quad . \tag{2.4}$$

Letting $X\, e^{j\phi_X} = \frac{A}{B}$, $Z\, e^{j\phi_Z} = C$ and $|\Gamma_L|\, e^{j\phi_L} = \Gamma_L$ we are able to write (2.4) as

$$\frac{b_3}{b_4} = B \frac{Xe^{j\phi_X}\,|\Gamma_L|e^{j\phi_L} + 1}{Ze^{j\phi_Z}\,|\Gamma_L|e^{j\phi_L} + 1} \quad . \tag{2.5}$$

The product of (2.5) with its complex conjugate yields the following power ratio,

$$\frac{P_3}{P_4} = \frac{b_3 b_3^*}{b_4 b_4^*} = |B|^2 \frac{X^2|\Gamma_L|^2 + 1 + 2X\,|\Gamma_L| \cos(\phi_X + \phi_L)}{Z^2|\Gamma_L|^2 + 1 + 2Z\,|\Gamma_L| \cos(\phi_Z + \phi_L)} \quad . \tag{2.6}$$

Since the power ratio equations for ports 5 and 6 are of identical form, we get the general equation

$$\frac{P_i}{P_R} = |B_i|^2 \frac{X_i^2|\Gamma_L|^2 + 1 + 2X_i|\Gamma_L| \cos(\phi_{xi} + \phi_L)}{Z^2|\Gamma_L|^2 + 1 + 2Z\,|\Gamma_L| \cos(\phi_Z + \phi_L)} \quad . \tag{2.7}$$

This equation is used in many applications of six-port theory and will be referred to as the six-port equation.

2.2 NEW CALIBRATION PROCEDURE

The degree to which a six-port can make precise reflection coefficient measurements depends on the accurate determination of the calibration constants and accurate power meter readings. This section presents a calibration procedure which minimizes errors due to power readings or other system imperfections. The procedure was developed by J. Dobrowolski et al., [3].

2.2.1 Calibration Standards

In chapter I several six-port systems were discussed. The system developed by Girimaji [11] worked well, but the four reflection calibration standards had to take on specific values of Γ_L = 1, -1, j, -j. These loads were implemented by cutting and shorting specific lengths of coaxial cable such that the electrical lengths fulfilled the input reflection coefficient requirement at the calibration frequency. The task of cutting and trimming exact lengths of line is difficult at best. This also caused problems in broadbanding the instrument because the phase of the reflection standards quite obviously change with frequency. In the calibration procedure presented here, the reflection standards can be of arbitrary (but known) electrical length. Dobrowolski [3] shows that the optimum phase separation between the standards is 90°. As such four short circuited lines were cut from coaxial line so that at the

center frequency the reflection standards were approximately 1, -1, j and -j. The exact phase was measured on a slotted line at the center frequency and any changes in phase due to changes in frequency could easily be calculated. Thus the six-port can be easily calibrated at a new frequency using the same calibration standards.

The phases of the standards were measured on a slotted line using an SMA short circuited connection to establish a reference plane on the test port of the five-port junction. The measured phases in radians at 1 GHz were as follows: $\phi_0 = 0.433\pi$, $\phi_1 = \pi$, $\phi_2 = -0.558\pi$ and $\phi_3 = -0.058\pi$. If we consider a Smith Chart representation, as in figure 2.1, we can calculate the physical length X_j or the electrical length ϕ_j at any frequency using

$$\frac{(\pi - \phi_j)}{2\pi} = \frac{X_j}{\lambda_0 / 2} \quad . \tag{2.8}$$

$\pi - \phi_j$ is the clockwise angle of the standard j from the short circuit position on the Smith Chart. Initially, at the center frequency, we can calculate the physical length X_j of each reflection standard using (2.8) and the slotted line phase measurements ϕ_j, j=0,1,2,3. When the frequency (hence wavelength) changes, we can calculate the new phase angle of the reflection standards by replacing λ_0 by the new wavelength, X_j by the value previously calculated and solving (2.8) for ϕ_j.

The Smith Chart of figure 2.1 shows the phase of each standard for the frequency range 900 to 1100 MHz in 50 MHZ intervals.

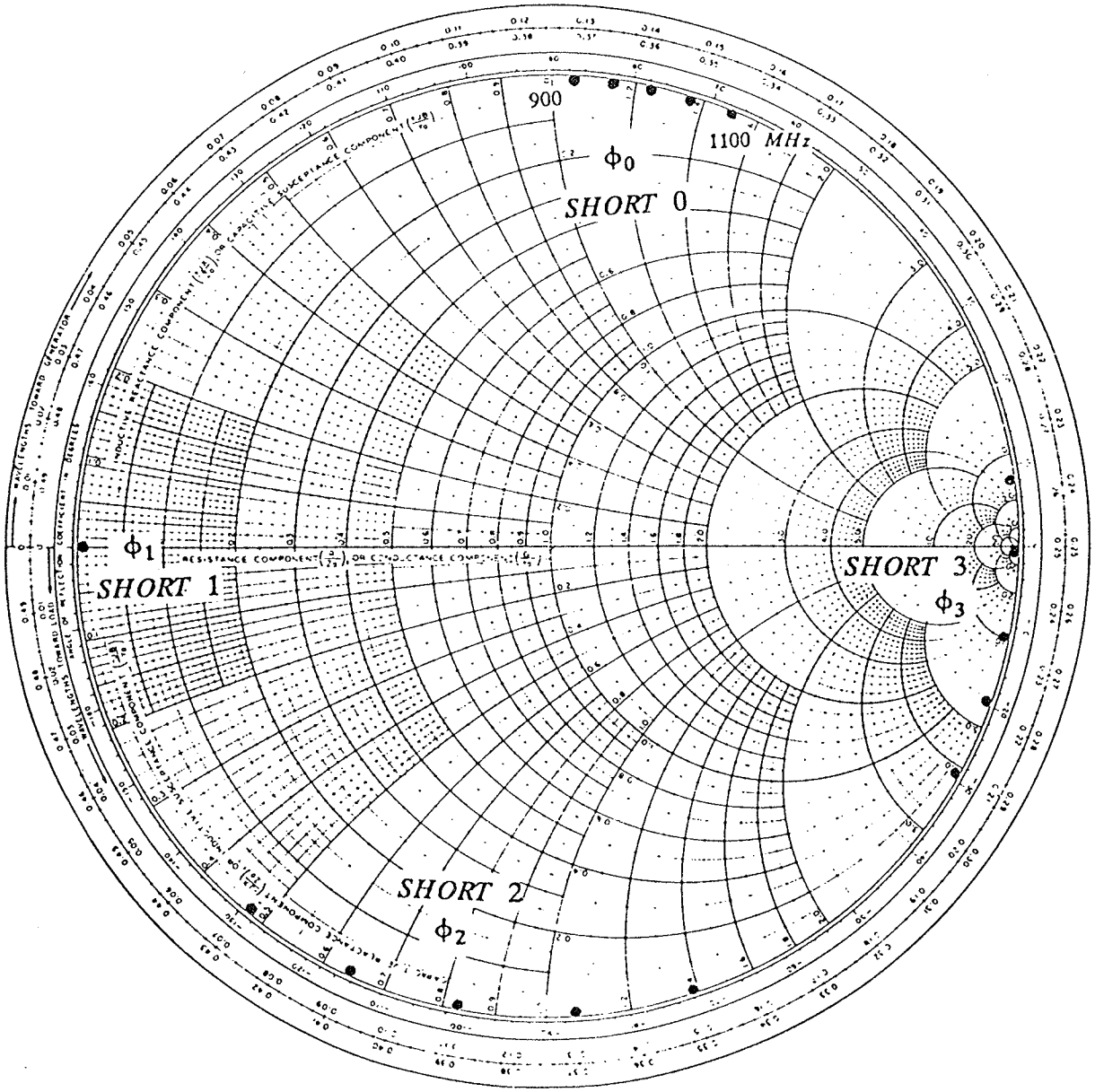

Figure 2.1: Phases of Reflection Standards

2.2.2 Calibration

The equation relating the power readings and the six port constants was found in section 2.1 to be

$$\frac{P_i}{P_R} = |B_i|^2 \frac{X_i^2 |\Gamma_L|^2 + 1 + 2 X_i |\Gamma_L| \cos(\phi_{ix} + \phi_L)}{Z^2 |\Gamma_L|^2 + 1 + 2 Z |\Gamma_L| \cos(\phi_L + \phi_Z)} \quad . \tag{2.9}$$

The power readings will of course differ from the actual power (due to detector inaccuracies etc.). The calibration technique to be described will attempt to minimize these errors. First a matrix equation will be derived from (2.9) and then an iterative procedure, used to minimize errors, will be presented.

For a given load $\Gamma_L = |\Gamma_L| \angle \phi_L$ applied to the six-port we obtain three detector power readings $P_i, i=1,2,3$; as well as a reading of the reference power P_R. If we apply a matched load ($\Gamma_L = 0$) we see from (2.9) that the constants $|B_i|$ can easily be determined. It will be shown that the balance of the constants in (2.9) can be determined by applying four unit magnitude reflection offsets of known phase (ϕ_j , j=0,1,2,3). Each detector power reading can be normalized by dividing by the reference power and the appropriate $|B_i|$. For detector index i=1,2,3 and calibration standard index j=0,1,2,3 this is

$$R_{ij} = \frac{P_i}{P_R \ |B_i|^2} \quad . \tag{2.10}$$

The twelve normalized powers R_{ij} so obtained are the basis for determining the final calibration constants.

If we expand (2.9) using (2.10) for a particular known offset short ($|\Gamma_L| = 1$) we get

$$R_{ij}\,[\,1 + 2Z\cos(\phi_Z + \phi_j) + Z^2\,] = 1 + 2X_i\cos(\phi_{xi} + \phi_j) + X_i^2 \quad . \tag{2.11}$$

Expanding the cosine terms gives

$$\begin{aligned} &R_{ij}\,[\,1 + 2Z\,\cos\phi_Z\,\cos\phi_j - 2Z\,\sin\phi_Z\,\sin\phi_j + Z^2\,] \\ &= 1 + 2X_i\,\cos\phi_{xi}\,\cos\phi_j - 2X_{xi}\,\sin\phi_{xi}\,\sin\phi_j + X_i^2 \quad . \end{aligned} \tag{2.12}$$

For i=1,2,3 and j=0,1,2,3 the resulting twelve equations can be written in matrix form.

For j=0 and i=1,2,3 :

$$\begin{aligned} &\begin{bmatrix} R_{10} & 2R_{10}\cos\phi_0 & -2R_{10}\sin\phi_0 \\ R_{20} & 2R_{20}\cos\phi_0 & -2R_{20}\sin\phi_0 \\ R_{30} & 2R_{30}\cos\phi_0 & -2R_{30}\sin\phi_0 \end{bmatrix} \begin{bmatrix} Z^2 \\ Z\cos\phi_Z \\ Z\sin\phi_Z \end{bmatrix} + \begin{bmatrix} R_{10} - 1 \\ R_{20} - 1 \\ R_{30} - 1 \end{bmatrix} \\ &= \begin{bmatrix} X_1^2 & X_1\cos\phi_{X1} & X_1\sin\phi_{X1} \\ X_2^2 & X_2\cos\phi_{X2} & X_2\sin\phi_{X2} \\ X_3^2 & X3\cos\phi_{X3} & X3\sin\phi_{X3} \end{bmatrix} \begin{bmatrix} 1 \\ 2\cos\phi_0 \\ -2\sin\phi_0 \end{bmatrix} \end{aligned} \tag{2.13}$$

or

$$\underline{A}\ \underline{z} + \underline{c} = [\underline{x}_1\ \underline{x}_2\ \underline{x}_3]^T\ \underline{b}_0 \tag{2.14}$$

where the elements of (2.14) are defined by direct comparison with (2.13). For j=1,2,3 and i=1,2,3 :

$$\begin{bmatrix} R_{i1} & 2R_{i1}\cos\phi_1 & -2R_{i1}\sin\phi_1 \\ R_{i2} & 2R_{i2}\cos\phi_2 & -2R_{i2}\sin\phi_2 \\ R_{i3} & 2R_{i3}\cos\phi_3 & -2R_{i3}\sin\phi_3 \end{bmatrix} \begin{bmatrix} Z^2 \\ Z\cos\phi_Z \\ Z\sin\phi_Z \end{bmatrix} + \begin{bmatrix} R_{i1}-1 \\ R_{i2}-1 \\ R_{i3}-1 \end{bmatrix}$$

$$= \begin{bmatrix} 1 & 2\cos\phi_1 & -2\sin\phi_1 \\ 1 & 2\cos\phi_2 & -2\sin\phi_2 \\ 1 & 2\cos\phi_3 & -2\sin\phi_3 \end{bmatrix} \begin{bmatrix} X_i^2 \\ X_i\cos\phi_{xi} \\ X_i\sin\phi_{xi} \end{bmatrix} \tag{2.15}$$

or

$$\underline{A}_i\ \underline{z} + \underline{c}_i = [\underline{b}_1\ \underline{b}_2\ \underline{b}_3]^T\ \underline{x}_i \tag{2.16}$$

where, again, the elements of (2.16) are defined by direct comparison with (2.15).

These four sets of simultaneous equations can be solved for the four unknown vectors $\underline{z}$, $\underline{x}_1$, $\underline{x}_2$ and $\underline{x}_3$. We obtain $\underline{x}_i$ by letting $\underline{B} = [\underline{b}_1\ \underline{b}_2\ \underline{b}_3]^T$ in (2.16) and by appropriately post multiplying, thus

$$\underline{x}_i = \underline{B}^{-1}\ (\underline{A}_i\underline{z} + \underline{c}_i)\ . \tag{2.17}$$

A substitution of (2.17) into (2.14) yields

$$\underline{A}\underline{z} + \underline{c} = [\underline{B}^{-1}(\underline{A}_1\underline{z} + \underline{c}_1)\ \underline{B}^{-1}(\underline{A}_2\underline{z} + \underline{c}_2)\ \underline{B}^{-1}(\underline{A}_3\underline{z} + \underline{c}_3)]^T\ \underline{b}_0\ . \tag{2.18}$$

Some further matrix manipulations (see appendix B) casts this equation into the form

$$\underline{Az} + \underline{c} = [\underline{A}_1\underline{z} \;\; \underline{A}_2\underline{z} \;\; \underline{A}_3\underline{z}]^T \;\; (\underline{B}^{-1})^T \;\; \underline{b}_0 + [\underline{c}_1 \;\; \underline{c}_2 \;\; \underline{c}_3]^T \;\; (\underline{B}^{-1})^T \;\; \underline{b}_0 \; . \qquad (2.19)$$

Finally, letting

$$\underline{\gamma} = (\underline{B}^{-1})^T \;\; \underline{b}_0 = \begin{bmatrix} \gamma_1 \\ \gamma_2 \\ \gamma_3 \end{bmatrix} \; .$$

With placement of $\underline{\gamma}$ in (2.19) we get

$$\underline{Az} + \underline{c} = [\underline{A}_1\underline{z} \;\; \underline{A}_2\underline{z} \;\; \underline{A}_3\underline{z}]^T \;\; \underline{\gamma} + [\underline{c}_1 \;\; \underline{c}_2 \;\; \underline{c}_3]^T \;\; \underline{\gamma} \; . \qquad (2.20)$$

Now we can manipulate equation (2.20) to enable us to solve for the $\underline{z}$ vector. From this we can find Z and ϕ_Z.

The first term on the right hand side of (2.20), after substituting R_{ij} and exposing the $\underline{z}$ vector, becomes

$$[\underline{A}_1\underline{z} \;\; \underline{A}_2\underline{z} \;\; \underline{A}_3\underline{z}]^T \;\; \underline{\gamma} =$$

$$\begin{bmatrix} R_{11}\gamma_1 + R_{12}\gamma_2 + R_{13}\gamma_3 & 2R_{11}\cos\phi_1\gamma_1 + 2R_{12}\cos\phi_2\gamma_2 + 2R_{13}\cos\phi_3\gamma_3 \\ R_{21}\gamma_1 + R_{22}\gamma_2 + R_{23}\gamma_3 & 2R_{21}\cos\phi_1\gamma 1 + 2R_{22}\cos\phi_2\gamma_2 + 2R_{23}\cos\phi_3\gamma_3 \\ R_{31}\gamma_1 + R_{32}\gamma_2 + R_{33}\gamma 3 & 2R_{31}\cos\phi_1\gamma_1 + 2R_{32}\cos\phi_2\gamma_2 + 2R_{33}\cos\phi_3\gamma_3 \end{bmatrix}$$

$$\begin{bmatrix} -2R_{11}\sin\phi_1\gamma_1 - 2R_{12}\sin\phi_2\gamma_2 - 2R_{13}\sin\phi_3\gamma_3 \\ -2R_{21}\sin\phi_1\gamma_1 - 2R_{22}\sin\phi_2\gamma_2 - 2R_{23}\sin\phi_3\gamma_3 \\ -2R_{31}sib\,\phi_1\gamma_1 - 2R_{32}\sin\phi_2\gamma_2 - 2R_{33}\sin\phi_3\gamma_3 \end{bmatrix} \begin{bmatrix} z_1 \\ z_2 \\ z_3 \end{bmatrix} = \underline{D} \; \underline{z} \; . \qquad (2.21)$$

The second term on the right hand side of (2.20), including $\underline{c}$ from the left hand side, becomes

$$[\underline{c}_1\ \underline{c}_2\ \underline{c}_3]^T\ \underline{\gamma} - \underline{c} = -\begin{bmatrix} R_{10} - (R_{11}\gamma_1 + R_{12}\gamma_2 + R_{13}\gamma_3) \\ R_{20} - (R_{21}\gamma_1 + R_{22}\gamma_2 + R_{23}\gamma_3) \\ R_{30} - (R_{31}\gamma_1 + R_{32}\gamma_2 + R_{33}\gamma_3) \end{bmatrix} = \underline{d} \quad . \tag{2.22}$$

Using (2.21) and (2.22) we can write (2.20) as

$$\begin{aligned} \underline{Az} &= \underline{Dz} + \underline{d} \quad , \\ [\underline{A} - \underline{D}]\,\underline{z} &= \underline{d} \quad , \\ \underline{Mz} &= \underline{d} \end{aligned} \tag{2.23}$$

where the elements of M are found from (2.13) and (2.21).

Now that an equation has been determined for $\underline{Z}$ we can use it to solve for Z while minimizing the errors. Defining an error vector as $\underline{\Psi}$ such that

$$\underline{\psi} = \underline{M}\ \underline{z} - \underline{d} \quad . \tag{2.24}$$

Noting that $z_1 = z_2^2 + z_3^2$, $d_1 = -M_{11}$, $d_2 = -M_{21}$, and $d_3 = -M_{31}$ we are able to write

$$\underline{\Psi} = \begin{bmatrix} M_{11} & M_{12} & M_{13} \\ M_{21} & M_{22} & M_{23} \\ M_{31} & M_{32} & M_{33} \end{bmatrix} \begin{bmatrix} z_2^2 + z_3^2 \\ z_2 \\ z_3 \end{bmatrix} + \begin{bmatrix} M_{11} \\ M_{12} \\ M_{13} \end{bmatrix} \tag{2.25}$$

or

$$\begin{aligned}\psi_1 &= M_{11}(1 + z_2^2 + z_3^2) + M_{12}z_2 + M_{13}z_3 \ , \\ \psi_2 &= M_{21}(1 + z_2^2 + z_3^2) + M_{22}z_2 + M_{23}z_3 \ , \\ \psi_3 &= M_{31}(1 + z_2^2 + z_3^2) + M_{32}z_2 + M_{23}z_3 \ .\end{aligned} \tag{2.26}$$

A measure of the total errors of the system is

$$E = \psi^T \psi = \psi_1^2 + \psi_2^2 + \psi_3^2 \tag{2.27}$$

which will be minimized for

$$\begin{aligned}\frac{\partial E}{\partial z_2} &= 2\psi_1 \frac{\partial \psi_1}{\partial z_2} + 2\psi_2 \frac{\partial \psi_2}{\partial z_2} + 2\psi_3 \frac{\partial \psi_3}{\partial z_2} = 0 \ , \\ \frac{\partial E}{\partial z_3} &= 2\psi_1 \frac{\partial \psi_1}{\partial z_3} + 2\psi_2 \frac{\partial \psi_2}{\partial z_3} + 2\psi_3 \frac{\partial \psi_3}{\partial z_3} = 0 \ .\end{aligned} \tag{2.28}$$

Performing the above partial differentiations on (2.26) we obtain

$$\begin{aligned}Q_2 = \frac{\partial E}{\partial z_2} &= 2az_2^2 + 2az_2z_3^2 + 3bz_2^2 + bz_3^2 + 2cz_2z_3 + z_2(e + 2a) + gz_3 + b = 0 \ , \\ Q_3 = \frac{\partial E}{\partial z_3} &= 2az_3^2 + 2az_2^2z_3 + 3cz_3^2 + cz_2^2 + 2bz_2z_3 + z_3(k + 2a) + gz_2 + c = 0\end{aligned} \tag{2.29}$$

where

$$a = M_{11}^2 + M_{21}^2 + M_{31}^2$$

$$b = M_{11}M_{12} + M_{21}M_{22} + M_{31}M_{32}$$

$$c = M_{11}M_{13} + M_{21}M_{23} + M_{31}M_{33}$$

$$e = M_{12}^2 + M_{22}^2 + M_{32}^2$$

$$g = M_{12}M_{13} + M_{22}M_{23} + M_{32}M_{33}$$

$$k = M_{13}^2 + M_{23}^2 + M_{33}^2 \quad .$$

Equations (12.29) form a set of two equations in two unknowns (z_2 and z_3). We can find the roots of these equations using the generalized Newton's iterative procedure as found in [13] . The iterative equations are

$$z_2^{(k+1)} = z_2^{(k)} - \frac{1}{D}\left[Q_2 \frac{\partial Q_3}{\partial z_3} - Q_3 \frac{\partial Q_2}{\partial z_3}\right]_{z_2^{(k)}, z_3^{(k)}} , \tag{2.30}$$

$$z_3^{(k+1)} = z_3^{(k)} - \frac{1}{D}\left[Q_3 \frac{\partial Q_2}{\partial z_2} - Q_2 \frac{\partial Q_3}{\partial z_2}\right]_{z_2^{(k)}, z_3^{(k)}} \tag{2.31}$$

where

$$D = \left[\frac{\partial Q_2}{\partial z_2}\frac{\partial Q_3}{\partial z_3} - \frac{\partial Q_2}{\partial z_3}\frac{\partial Q_3}{\partial Q_2}\right]_{z_2^{(k)}, z_3^{(k)}} .$$

Iterations k are performed until the results converge. As an initial estimate of z_2 and z_3 we can use any two of (2.26), setting the error vector to zero. This gives

$$\begin{aligned} M_{11}(z_1 + 1) + M_{12}z_2 + M_{13}z_3 = 0 \quad , \\ M_{21}(z_1 + 1) + M_{22}z_2 + M_{23}z_3 = 0 \quad . \end{aligned} \tag{2.32}$$

If we multiply the first by M_{12} and the second by M_{11} we can eliminate $(z_1 + 1)$ and get

$$\frac{z_3}{z_2} = \frac{M_{12}M_{21} - M_{11}M_{22}}{M_{23}M_{11} - M_{21}M_{13}} \quad .$$

From (2.13) we know that $z_1 = Z^2$, $z_2 = Z\cos\phi_z$ and $z_3 = Z\sin\phi_z$ so that

$$\phi_Z = TAN^{-1}\left[\frac{M_{12}M_{21} - M_{11}M_{22}}{M_{23}M_{11} - M_{21}M_{13}}\right] \quad . \tag{2.33}$$

The 180° ambiguity in the inverse tangent function can be resolved by using the first equation of (2.32) with appropriate substitutions for z_1, z_2 and z_3 , thus

$$M_{11}(Z^2 + 1) + M_{12}Z\cos\phi_Z + M_{13}Z\sin\phi_Z = 0$$

or

$$Z^2 + 1 + Z\left[\frac{M_{12}\cos\phi_z + M_{13}\sin\phi_z}{M_{11}}\right] = 0 \quad . \tag{2.34}$$

If we let X be the bracketed term in this equation then

$$Z^2 - Z\,X + 1 = 0$$

for which the solution is

$$Z = \frac{X \pm \sqrt{X^2 - 4}}{2} \quad . \tag{2.35}$$

Because Z has to be real, $X^2 - 4 \geq 0$, and we require

$$X \geq 2 \quad . \tag{2.36}$$

Now we can use (2.33) to find ϕ_Z and solve for X. If (2.36) is violated, we know that we must add 180° to the

value of ϕ_z. Z can be found by employing (2.35). Riblet and Hansson address the problem of the $\pm$ sign in (2.35) in [5]. They find that $Z < 1$ so the negative sign must be taken.

Discontinuities in the inverse tangent function can be resolved by writing (2.33) as

$$\phi_Z = TAN^{-1}\left[\frac{\sin\phi_Z}{\cos\phi_Z}\right] = TAN^{-1}\left[\frac{Z_3}{Z_2}\right] \tag{2.37}$$

and noting the following:

$$\begin{aligned} Z_3 = 0, Z_2 > 0 &\rightarrow \phi_Z = 0 \\ Z_3 = 0, Z_2 < 0 &\rightarrow \phi_Z = \pi \\ Z_3 > 0, Z_2 = 0 &\rightarrow \phi_Z = \pi/2 \\ Z_3 < 0, Z_2 = 0 &\rightarrow \phi_Z = -\pi/2 \end{aligned}$$

Now that Z and ϕ_Z are known, we can use (2.16) to solve for X_i; i=1,2,3. Write (2.16) as

$$\underline{Bx_i} = \underline{A_i} z + \underline{c_i} = \underline{U_i} \quad . \tag{2.38}$$

For the imperfect system we have an error vector $\underline{\eta}$ such that

$$\underline{\eta} = [\eta_1\ \eta_2\ \eta_3]^T = \underline{Bx_i} - \underline{U_i} \quad . \tag{2.39}$$

We can follow the same procedure as for Z by letting the error function F be

$$F = \eta_1^2 + \eta_2^2 + \eta_3^2 \tag{2.40}$$

and minimizing it as

$$\frac{\partial F}{\partial x_{i2}} = 2\eta_1\frac{\partial \eta_1}{\partial x_{i2}} + 2\eta_2\frac{\partial \eta_2}{\partial x_{i2}} + 2\eta_3\frac{\partial \eta_3}{\partial x_{i2}} = 0 \quad ,$$

$$\frac{\partial F}{\partial x_{i3}} = 2\eta_1\frac{\partial \eta_1}{\partial x_{i3}} + 2\eta_2\frac{\partial \eta_2}{\partial x_{i3}} + 2\eta_3\frac{\partial \eta_3}{\partial x_{i3}} = 0 \quad . \tag{2.41}$$

Performing the above partial differentiations we have

$$\begin{aligned} L_2 = \frac{\partial F}{\partial x_{i2}} &= 6x_{i2}^3 + 6x_{i2}x_{i3}^2 + 6ax_{i2}^2 + 2ax_{i3}^2 - 4bx_{i2}x_{i3} \\ &+ 2(2g - Z^2d_i - 2Z\cos\phi_z v_i + 2Z\sin\phi_z e_i - d_i + 3)x_{i2} - 4sx_{i3} \\ &+ 2(a - v_i - Z^2v_i + 2Z\sin\phi_z k_i - 2Z\cos\phi_z t_i) \quad , \end{aligned} \tag{2.42}$$

$$\begin{aligned} L_3 = \frac{\partial F}{\partial x_{i3}} &= 6x_{i3}^3 + 6x_{i2}^2x_{i3} - 6bx_{i3}^2 - 2bx_{i2}^2 + 4ax_{i3}x_{i2} \\ &+ 2(2u - Z^2d_i - 2Z\cos\phi_z v_i + 2Z\sin\phi_z e_i - d_i + 3)x_{i3} - 4sx_{i2} \\ &- 2(b - e_i - Z^2e_i + 2Z\sin\phi_z n_i - 2Z\cos\phi_z k_i) \end{aligned}$$

where

$$a = \cos\phi_1 + \cos\phi_2 + \cos\phi_3$$

$$b = \sin\phi_1 + \sin\phi_2 + \sin\phi_3$$

$$g = \cos^2\phi_1 + \cos^2\phi_2 + \cos^2\phi_3$$

$$d_i = R_{i1} + R_{i2} + R_{i3}$$

$$e_i = R_{i1}\sin\phi_1 + R_{i2}\sin\phi_2 + R_{i3}\sin\phi_3$$

$$v_i = R_{i1}\cos\phi_1 + R_{i2}\cos\phi_2 + R_{i3}\cos\phi_3$$

$$s = \sin\phi_1\cos\phi_1 + \sin\phi_2\cos\phi_2 + \sin\phi_3\cos\phi_3$$

$$t_i = R_{i1}\cos^2\phi_1 + R_{i2}\cos^2\phi_2 + R_{i3}\cos^2\phi_3$$

$$k_i = R_{i1}\sin\phi_1\cos\phi_1 + R_{i2}\sin\phi_2\cos\phi_2 + R_{i3}\sin\phi_3\cos\phi_3$$

$$u = \sin^2\phi_1 + \sin^2\phi_2 + \sin^2\phi_3$$

$$n_i = R_{i1}\sin^2\phi_1 + R_{i2}\sin^2\phi_2 + R_{i3}\sin^2\phi_3 \quad .$$

The same iterative procedure is used to solve equations (2.41) where the iterative formulas are

$$x_{i2}^{(k+1)} = x_{i2}^{(k)} - \frac{1}{D}\left[L_2\frac{\partial L_3}{\partial x_{i3}} - L_3\frac{\partial L_2}{\partial x_{i3}}\right]_{x_{i2}^{(k)},\, x_{i3}^{(k)}},$$

$$x_{i3}^{(k+1)} = x_{i3}^{(k)} - \frac{1}{D}\left[L_3\frac{\partial L_2}{\partial x_{i2}} - L_2\frac{\partial L_3}{\partial x_{i2}}\right]_{x_{i2}^{(k)},\, x_{i3}^{(k)}} \qquad (2.43)$$

where

$$D = \left[\frac{\partial L_2}{\partial x_{i2}}\,\frac{\partial L_3}{\partial x_{i3}} - \frac{\partial L_2}{\partial x_{i3}}\,\frac{\partial L_3}{\partial x_{i2}}\right]_{x_{i2}^{(k)},\, x_{i3}^{(k)}} .$$

As an initial estimate we can solve for x_i in $\underline{B}x_i - \underline{U}_i = 0$ as was done for Z. All the calibration constants have now been determined and the next section will describe how Γ_L is calculated from a set of power readings when an unknown load is connected to the six-port system.

2.3 DETERMINATION OF Γ_L

Once we have the calibration constants we can use the six-port equation to solve for Γ_L. We can rewrite equation (2.7) in matrix form as follows:

$$\begin{bmatrix} S_{11} & S_{12} & S_{13} \\ S_{21} & S_{22} & S_{23} \\ S_{31} & S_{32} & S_{33} \end{bmatrix} \begin{bmatrix} |\Gamma_L|^2 \\ 2|\Gamma_L| \cos\phi_L \\ 2|\Gamma_L| \sin\phi_L \end{bmatrix} = \begin{bmatrix} 1 - \dfrac{P_1}{P_R B_1} \\ 1 - \dfrac{P_2}{P_R B_2} \\ 1 - \dfrac{P_3}{P_R B_3} \end{bmatrix} \tag{2.44}$$

where for i=1,2,3;

$$S_{i1} = \left(\frac{P_i}{P_R B_i}\right) Z^2 - X_i^2 \quad ,$$

$$S_{i2} = \left(\frac{P_i}{P_R B_i}\right) Z \cos\phi_Z - X_i \cos\phi_{xi} \quad ,$$

$$S_{i3} = X_i \sin\phi_{xi} - Z \left(\frac{P_i}{P_R B_i}\right) \sin\phi_Z \quad .$$

All of the S matrix coefficients are known from four simple power readings taken with the device connected to the test port. We can obtain Γ_L by post multiplying (2.44) by S^{-1} which gives $\Gamma_1 = |\Gamma_L|^2$, $\Gamma_2 = 2|\Gamma_L| \cos\phi_L$ and $\Gamma_3 = 2|\Gamma_L| \sin\phi_L$. These yield $|\Gamma_L| = (\Gamma_1)^{1/2}$ and $\phi_L = \mathrm{Tan}^{-1}(\Gamma_3 / \Gamma_2)$.

Chapter III

SIX-PORT IMPLEMENTATION

Now that we have discussed the six-port theory in detail we can proceed to describe the entire six-port system.

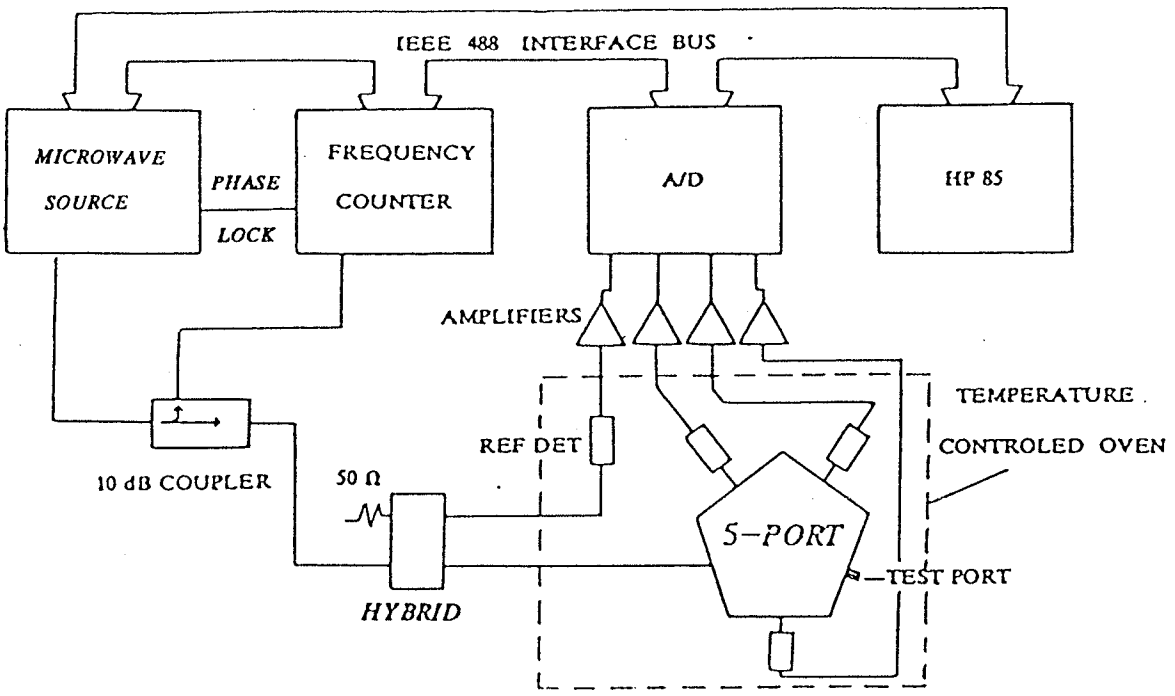

Figure 3.1: THE SIX-PORT SYSTEM

Figure 3.1 shows the components of the system. The HP 85 desk top computer controls the entire six-port process, in both calibration and measurement of Γ_L . All software is written in BASIC and keyboard interactions control the program flow.

Microwave power is supplied by an HP 8620 C mainframe equipped with a 0.01 to 2.4 GHz 86222B RF plug in. The frequency is controlled by an EIP model 371 source locking counter. The counter can phase lock the source to an accuracy of 10 Hz. The final component in the system is an HP 59313 A analogue to digital converter. This device is controlled by the HP 85 by means of an IEEE 488 interface bus. An analogue signal is converted to 11 bit two's compliment binary data which is transmitted in two eight bit bytes. Its input range is set to five volts maximum and conversion rates of up to 50 samples per second are possible.

The first step in preparing the system for use is to determine the calibration constants. The procedure is similar to Girimaji's [11] in that four offset shorts and a matched load are used to determine the constants. Once these calibration constants have been determined for a given frequency one is ready to make reflection coefficient measurements.

The rest of this chapter describes the major components of the system in more detail and introduces the system software.

3.1 THE SIX-PORT NETWORK

This section describes the components of the six-port network which has been developed. The heart of the system is a five way equal power division junction that is placed in tandem with a hybrid coupler used to provide the reference power port. The five-port junction was realized in stripline and operates at a center frequency of 1 GHz. Figure 3.2 shows the six-port network.

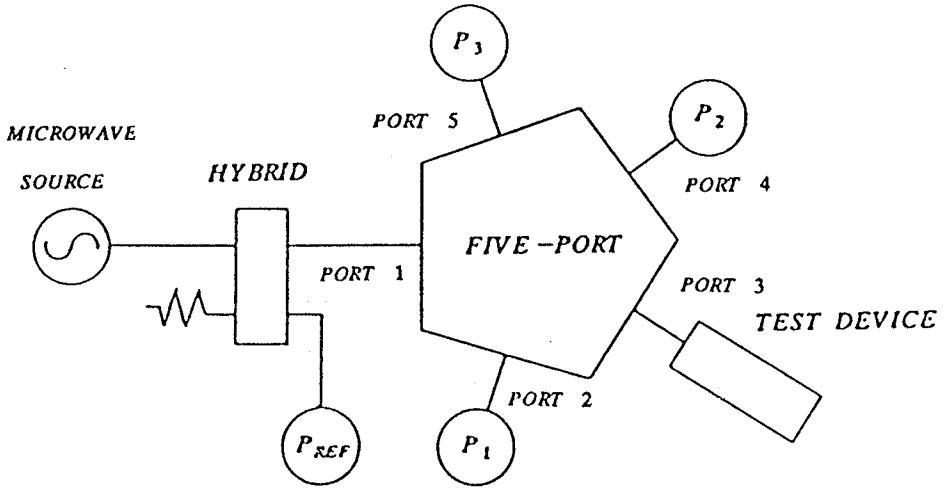

Figure 3.2: THE SIX PORT NETWORK

The powers P_i are measured by detector - amplifier - analogue to digital converter systems as shown in figure 3.3. Details of the power detection scheme are found in Chapter IV. A hybrid is used to couple power to the reference detector system. It provides good isolation between source and five-port and allows the reference detector to operate at the fairly high levels of the source

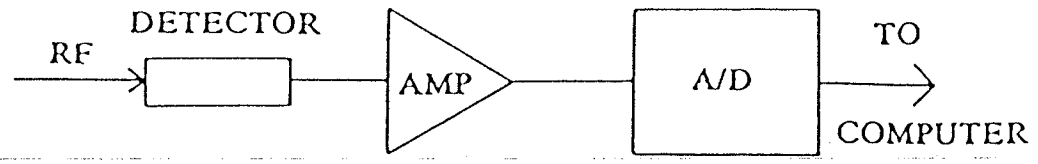

Figure 3.3: POWER DETECTION SCHEME

(0 to -5 dBm). A previous system [11] used a 10 dB directional coupler in place of the hybrid. It provided good isolation, but forced the reference detector to operate at -10 to -15 dBm levels. With this system the gain necessary to boost the dc detector output to the 0 to 5 volt A/D converter operating level was in the order of 500. This high gain caused unnecessary error in the system.

3.2 THE SYMMETRIC FIVE-PORT JUNCTION

This section deals with the five-port junction in greater detail. To begin with the junction is assumed to be reciprocal and perfectly matched. As such we can write for the elements of the scattering matrix that $S_{ij} = S_{ji}$ and $S_{ii} = 0$ for i=1...5. If we assume the junction to be lossless and observe the symmetry of the junction as labelled in figure 3.2, the junction scattering coefficients must be related as

$$\alpha = S_{12} = S_{23} = S_{34} = S_{45} = S_{15} , \tag{3.1}$$

$$\beta = S_{13} = S_{25} = S_{35} = S_{24} = S_{14} . \tag{3.2}$$

Applying the unitary property, we have

$$\begin{bmatrix} 0 & \alpha^* & \beta^* & \beta^* & \alpha^* \\ \alpha^* & 0 & \alpha^* & \beta^* & \beta^* \\ \beta^* & \alpha^* & 0 & \alpha^* & \beta^* \\ \beta^* & \beta^* & \alpha^* & 0 & \alpha_* \\ \alpha^* & \beta^* & \beta^* & \alpha^* & 0 \end{bmatrix} \begin{bmatrix} 0 & \alpha & \beta & \beta & \alpha \\ \alpha & 0 & \alpha & \beta & \beta \\ \beta & \alpha & 0 & \alpha & \beta \\ \beta & \beta & \alpha & 0 & \alpha \\ \alpha & \beta & \beta & \alpha & 0 \end{bmatrix} = \begin{bmatrix} 1 & 0 & 0 & 0 & 0 \\ 0 & 1 & 0 & 0 & 0 \\ 0 & 0 & 1 & 0 & 0 \\ 0 & 0 & 0 & 1 & 0 \\ 0 & 0 & 0 & 0 & 1 \end{bmatrix}$$

which yields

$$2|\alpha|^2 + 2|\beta|^2 = 1 \quad , \tag{3.3}$$

$$\beta^*\alpha + \alpha^*\beta + |\beta|^2 = 0 \quad , \tag{3.4}$$

$$\beta^*\alpha + \alpha^*\beta + |\alpha|^2 = 0 \quad . \tag{3.5}$$

Subtracting equation (3.5) from (3.4) we find that $|\alpha| = |\beta|$ which if placed in (3.3) yields $|\alpha| = \frac{1}{2}$. We can choose the reference planes so that $\alpha = \alpha^* = |\alpha|$ and use (3.4) and (3.5) to solve for β. Thus

$$\begin{aligned} &\beta^*\alpha + \alpha^*\beta + |\beta|^2 = 0 \quad , \\ &\alpha^*(\beta^* + \beta) = \alpha^2 \quad , \\ &\beta^*\beta = -\frac{1}{2} \quad . \end{aligned} \tag{3.6}$$

Letting $\beta = x + jy$ in the last equation of (3.6) gives

$$x - jy + x + jy = -\frac{1}{2} \tag{3.7}$$

which requires that $x = -1/4$. This result together with $|\beta|^2 = x^2 + y^2 = 1/4$ gives $y = \pm \frac{\sqrt{3}}{4}$. Therefore, for α real and positive we have

$$\beta = -1/4 \pm \frac{\sqrt{3}}{4} = \frac{1}{2} \angle \pm 120 \ .$$

Now that the scattering parameters of the five-port junction are known we can find the outgoing waves b_i from

$$[b] = [S]\,[a] \ . \tag{3.8}$$

Using these equations we could find P_1, P_2 and P_3 (where for instance $P_1 \alpha |b_1|^2$) and then follow the procedure set out by Engen [4] to find Γ_L by use of the q point equations (equations (1.9)). We have thus far assumed ideal properties, which are of course impossible to achieve in practice. Thus Γ_L determined in this way would only be an estimate.

The actual five-port is a ring type structure with five radial short circuited stubs as depicted in figure 3.4. The details of the design (for instance the strip widths etc.) will not be discussed here but may be found in [11]. In the band of interest (900 to 1100 MHz) the insertion loss for all ports was tested to be less than 7 dB (about 6.5 dB at the band center). See appendix H for a detailed graph . The return loss was better than -30 dB for all ports at the center frequency. On the band 975 to 1050 MHz the return loss was still better than -20 dB but only -10 dB at the

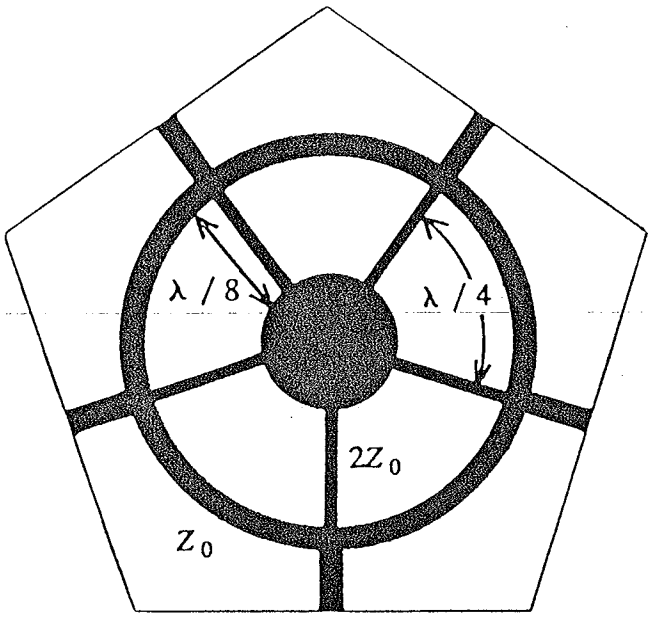

Figure 3.4: SYMMETRIC FIVE-PORT

band edges (see appendix H). These measurements show that the five-port junction is not ideal over the frequency band of interest. The new calibration procedure (described in chapter II) takes into account these imperfections as well as power measurement errors and calibrates the six-port as an imperfect device by minimizing the errors.

3.3 SYSTEM SOFTWARE

The software for the six-port reflectometer is broken up into two programs. The first program, "6CAL", performs the calibration procedure and the second, "GAMMA", calculates Γ_L. Both are written in BASIC and acquire data from the A/D converter through the IEEE 488 interface bus. Program listings are given in Appendix F.

3.3.1 6CAL PROGRAM

The 6CAL program uses the procedure outlined in chapter II to calculate the six port constants. A flowchart of the program is shown in figure 3.5. First the program prompts the user for the frequency of operation and the phases of the four offset shorts are calculated using equation (2.8). Then it prompts the user to connect a matched load to the test port and waits for a carriage return to begin sampling the detector voltages. Ten samples of each detector voltage are taken, and the average voltage for each is stored in a two dimensional array (with indicies for detector number and standard number). The offset shorts are then asked for one at a time and data is stored in the array. The power readings are found by using the characterization curves and normalization with respect to the reference power is done. The values obtained with the matched load are used to determine $|B_i|$ then the rest of the constants are calculated as described in the section (2.2). The final constants are printed out and stored in memory.

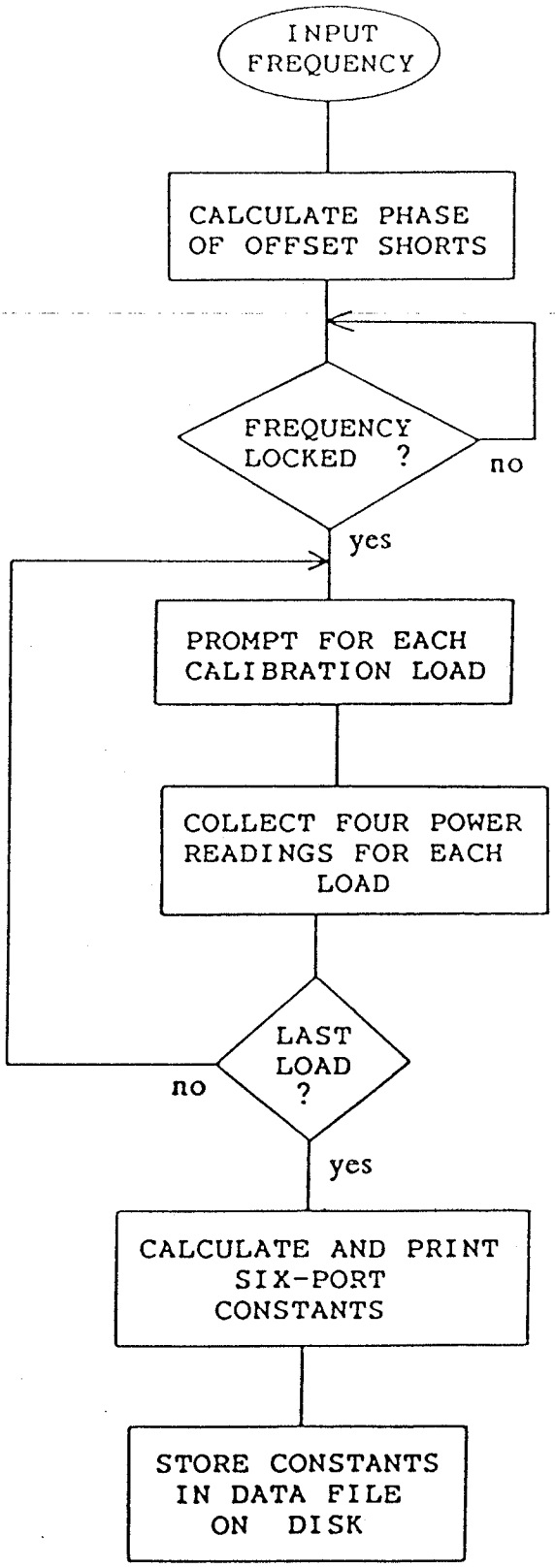

Figure 3.5: 6CAL FLOWCHART

3.3.2 GAMMA PROGRAM

The first step in GAMMA prompts the user for the frequency of operation. The six-port must be precalibrated for one or several operating frequencies. The appropriate calibration constants are taken from memory and the user is asked to lock the source at the required frequency. When a carriage control is received the program takes a ten sample average of each detector voltage. These voltages are converted to powers and equation (2.44) is used to find Γ_L. $|\Gamma_L|$ is printed as a four decimal place number between zero and one and Φ_L is printed as a three decimal place number in degrees. The program then loops back to the beginning to prepare for another measurement. Figure 3.6 shows a flowchart of the program.

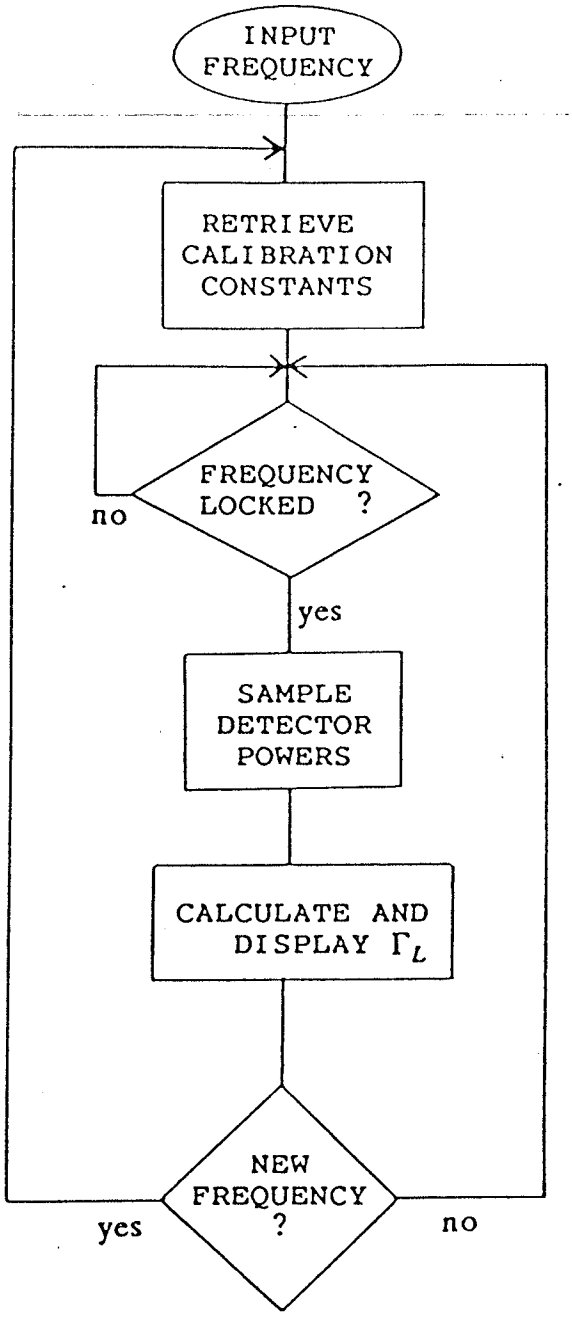

Figure 3.6: GAMMA FLOWCHART

Chapter IV

THE DETECTORS

In this chapter the power detection scheme is discussed. This includes a description of the diode detectors used, their temperature stabilization, the characterization procedure and a power tracking test.

The detectors used in this system are zero biased Schottky diodes made by Wiltron (Model 73 series). The specifications show a frequency response flatness of less than 0.5 dB over a 100 kHz to 4 GHz band. The maximum SWR is 1.2 where 1.1 is typical. As mentioned earlier, these detectors are used to measure power by using the set up of figure 3.3. Once the detectors have been characterized, an incident power can be found by applying the voltage sampled at the A/D (HP 59313 A) to the polynomial approximations. The process is computer controlled and sampling rates of up to 50 samples per second can be achieved. The amplifiers are simple type 741 inverting amplifiers with gains ranging from 40 to 100. The input noise to a typical amplifier was measured to be less than 0.1 mV and the output noise was between 6 and 9 mV on five volts full scale.

4.1 TEMPERATURE STABILITY

It is well known that the electrical characteristics of diode detectors change with temperature. This can be seen in the family of power versus voltage curves for detector 1 in figure 4.1. The output dc voltage verses input RF power has been plotted for several temperatures. A method for obtaining these curves is described in section 4.2.

Accurate power measurements can be made by stabilizing the temperature of the detectors and modeling the power versus voltage curves as high order polynomials. In the detection system, temperature stability is achieved by mounting the six-port along with its detectors in a temperature controlled oven. The oven consists of a 1/4 inch aluminum plate (approximately 25 by 30 cm) whose temperature is controlled by a type LN 3911 temperature controller . Surrounding the plate on all sides is about 3/4 inches of styrofoam. The five-port junction and associated detectors are mounted directly on to the plate along with the temperature controller, a power transistor and two high power resistors. A temperature sensor is built into the bottom of the ceramic package of the controller. The sensor voltage is compared with a reference voltage level set by a simple potentiometer circuit. The output of the controller gives a high dc voltage for temperatures below 0.5 degrees of the reference temperature, and a low voltage for temperatures above this range. This logic swing

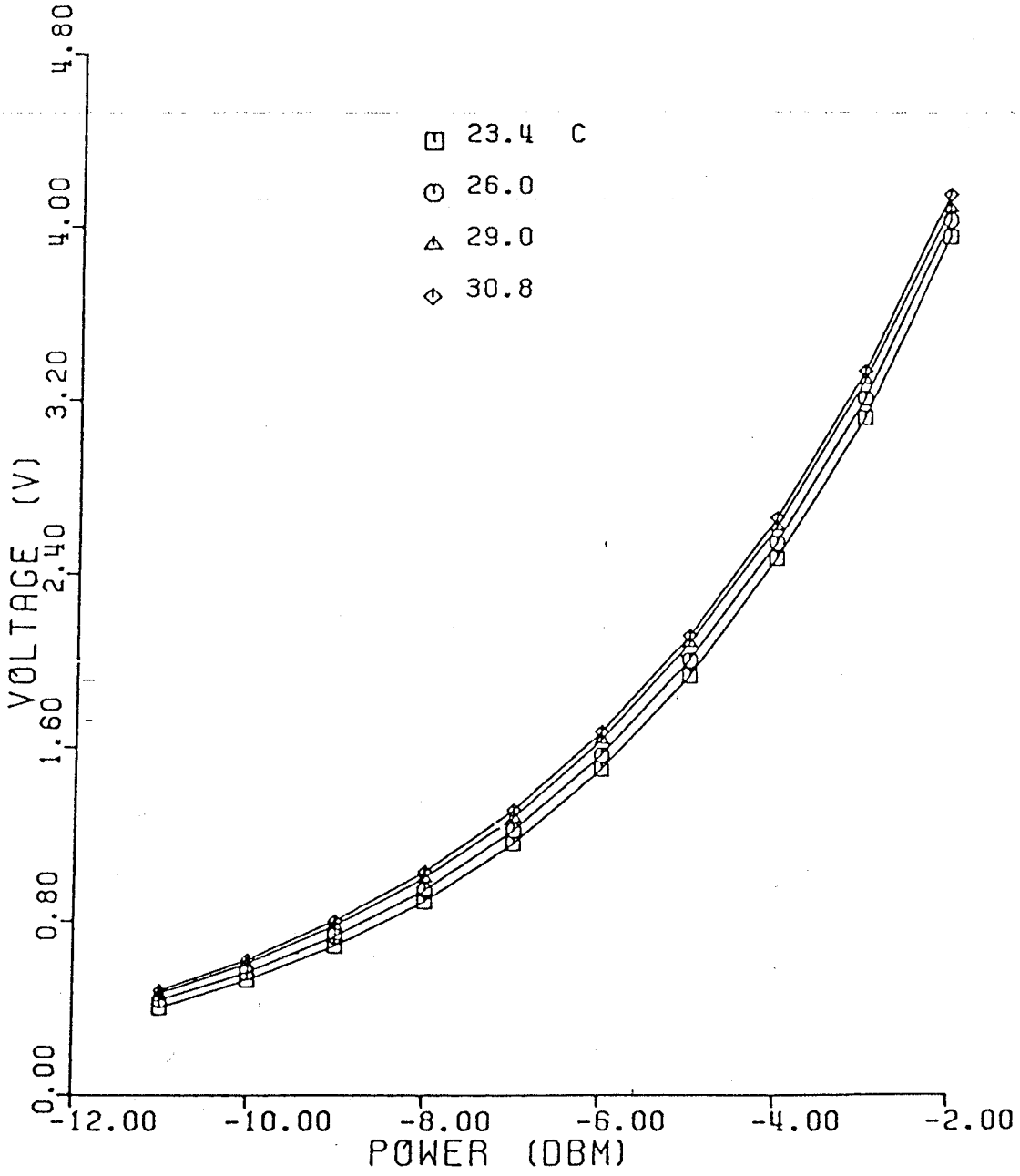

Figure 4.1: POWER VS. VOLTAGE WITH TEMPERATURE, DETECTOR 1

swing drives two amplifier stages which in turn drive the power transistor (NJ 311) mounted on the plate. The circuit is shown in figure 4.2.

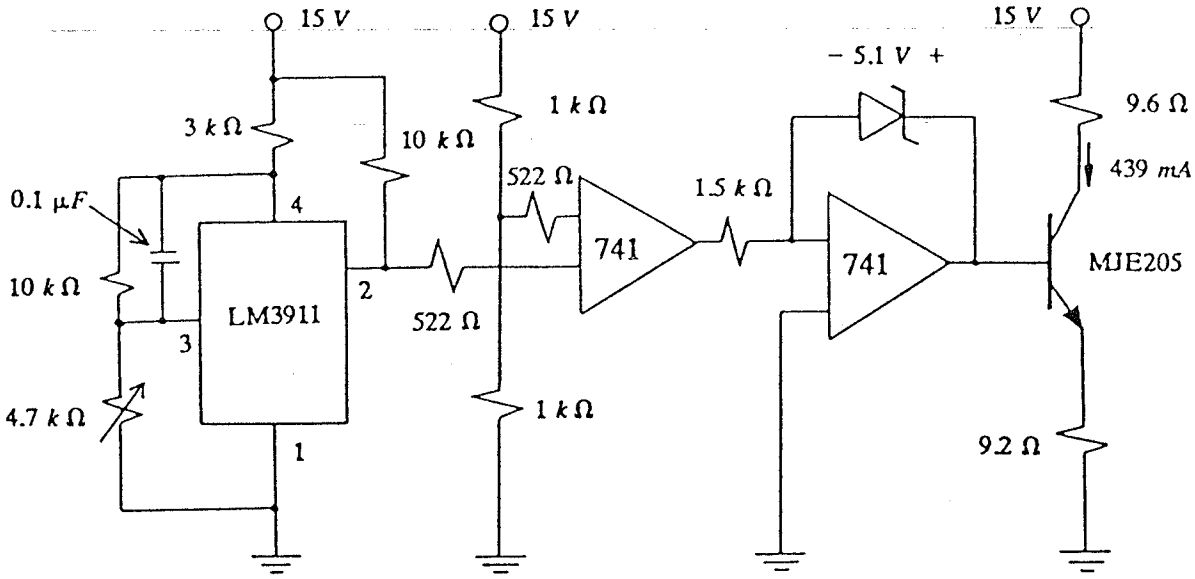

Figure 4.2: TEMPERATURE CONTROL CIRCUIT

The transistor supplies heat through the emitter and collector resistors as well as its own heat sink. The collector circuit dissipation is 2.62 watts, the emitter circuit 1.8 watts for a total of 4.42 watts. It takes about two hours for the plate temperature to stabilize.

4.2 DETECTOR CHARACTERIZATION

The detectors were characterized located in the temperature controlled oven at the stabilized temperature of $35 \pm 0.5^{\circ}C$. The first step in the characterization procedure is to estimate the range of powers expected to be applied to each detector. It has been shown that the six port equation relates the power at a given port i to the six port constants

$$\frac{P_i}{P_R} = |B_i|^2 \frac{X_i^2 |\Gamma_L|^2 + 1 + 2 X_i |\Gamma_L| \cos(\phi_{ix} + \phi_L)}{Z^2 |\Gamma_L|^2 + 1 + 2 Z |\Gamma_L| \cos(\phi_{L_r} + \phi_Z)} \quad . \tag{4.1}$$

Riblet and Hansson [5] have shown the ideal six-port constants to be as follows: $|B_i|^2 = 0.25$, $Z\, e^{j\phi_z} = 0$, $X_1\, e^{j\phi_{x1}} = \frac{1}{2}\, e^{-j\frac{\pi}{2}}$, $X_2\, e^{j\phi_{x2}} = \frac{1}{2}\, e^{j5\frac{\pi}{2}}$ and $X_3\, e^{j\phi_{x3}} = \frac{1}{2}\, e^{j\frac{\pi}{6}}$.

These values when used in equation (4.1) with the phase ϕ_L varied, but with $|\Gamma_L| = 1$, determine the range of the power delivered to the detectors. When ϕ_L is varied over 360° we find:

Detectors 1 and 2; Pmin = -12.5 dBm, Pmax = -2.5 dBm.

Detector 3; Pmin = -10.2 dBm, Pmax = -2.8 dBm.

Recall that these results are for an ideal six-port. To estimate how the detector powers of the actual six-port varied, the constants found by Girimaji [11] were used in

the same manner. These constants are: $Z = 0.051 \angle 266.7^{\circ}$, $X1 = 0.41 \angle 69.7^{\circ}$, $X2 = 0.52 \angle 197.7^{\circ}$, $X3 = 0.48 \angle -58.6^{\circ}$, $|B_1|^2 = 0.273$, $|B_2|^2 = 0.232$, $|B_3|^2 = 0.251$. When these constants are applied to (4.1) and ϕ_L is varied over 360° in 10 degree intervals with $|\Gamma_L| = 1$, we find the power extremes (for a reference power of 0 dBm) to be:

Detector 1; Pmin = -10.7 dBm, Pmax = -2.218 dBm

Detector 2; Pmin = -12.5 dBm, Pmax = -2.8 dBm

Detector 3; Pmin = -11.4 dBm, Pmax = -2.9 dBm

These extremes lead to a choice of -13 dBm to -2 dBm for the range of detectors 2 and 3 and -11 dBm to -2 dBm for detector 1. The same procedure was followed for $|\Gamma_L| = 0.8$ and $|\Gamma_L| = 0.2$ (where the phase ϕ_L was again varied over 360°). For these cases the minimum and maximum power levels for each detector were within the limits found for the $|\Gamma_L| = 1$ study. Full results for the complete study can be found in appendix C.

The power incident on the five-port is set to about 0 dBm so the range of 3 dBm to -5 dBm was chosen for the characterization of the reference detector.

For detectors 1,2 and 3 the circuit of figure 4.3 was used to collect power versus voltage data.

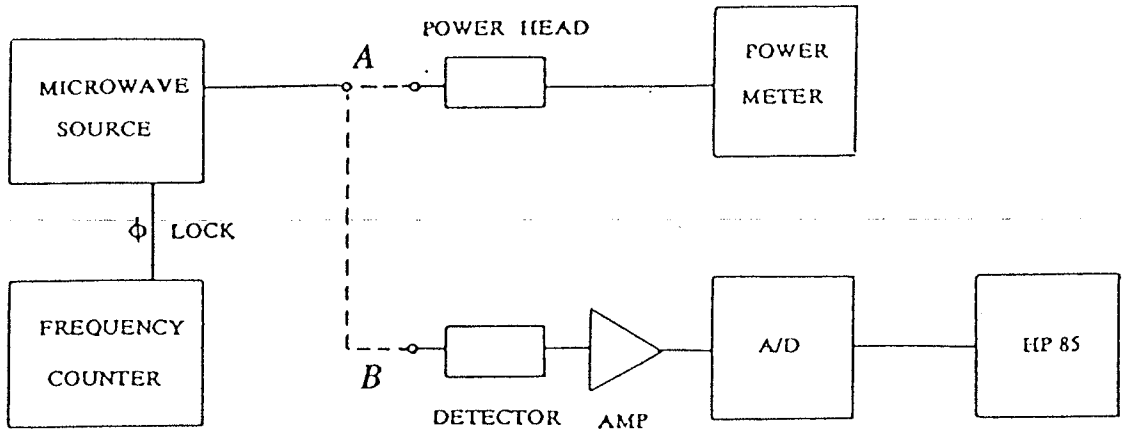

Figure 4.3: POWER VS. VOLTAGE MEASUREMENT

First the source is phase locked at the center frequency. A starting maximum power is measured with the power meter connected to the source at point A. Then the source is connected to point B and the voltage is sampled ten times by the A/D converter and the information is passed to the computer. The computer takes the average value of these ten samples and stores the information in an array along with the measured power. The power is then lowered 1 dB by monitoring with the power meter and the procedure is repeated until the entire range is covered. The SWR's of the detectors and the power sensor (HP model 8481 A) are very close ($1.1 < SWR < 1.2$ for both) so the method is laborious but accurate.

The procedure for characterizing the reference detector

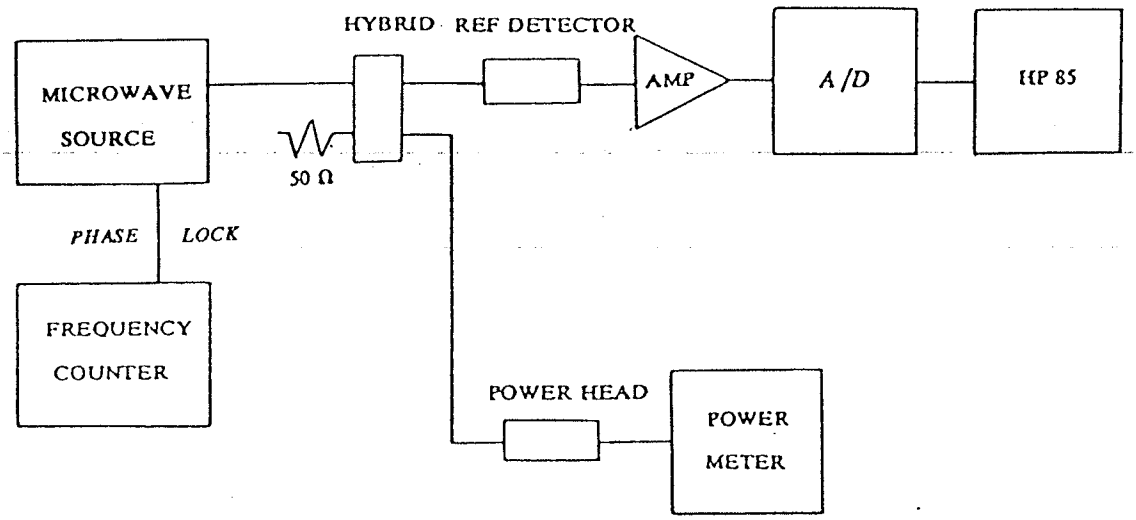

Figure 4.4: REF POWER VS. VOLTAGE MEASUREMENT

is somewhat different. Figure 4.4 shows the set up. The reference detector is in its proper place in the six-port system with the five-port junction replaced by the power sensor. Now the detector can be characterized such that its output voltage corresponds to the power incident on the five-port junction. Again the voltage and power are correlated in an array by the computer. The data collected for all four detectors is found in appendix D.

A curve fitting procedure will be applied to find the coefficients of a fourth order polynomial that best fits the power versus voltage data. Intuitively we can sense that the smaller the range of the curve, the more easily we can

fit the polynomial. For this reason, we have broken up the data for detectors 1, 2 and 3 into two subranges. That is there will be two polynomials for each of these detectors. By doing so the polynomials will fit the curves to ±0.01 dBm. When a polynomial was determined for the whole range, the accuracy was only about ±0.1 dBm. The range for the reference detector was small enough to have an accuracy of better than ±0.015 dBm with only one polynomial.

A Statistical Analysis Systems (SAS) routine called NLIN was used to determine the coefficients of the polynomials. NLIN uses a nonlinear regression procedure to produce the best least-squares estimates of the parameters. First NLIN evaluates the residual sum of the squares of each combination of a grid of starting values to determine the best place to start the iterative procedure. Then the Gauss - Newton iterative method is used to regress the residuals on the partial derivatives of the model with respect to the parameters until the iterations converge. More detail on the Gauss - Newton method can be found in [12]. Table 4.1 shows the results of the NLIN procedure for each detector. The model used for the procedure was

$$P = B5x^4 + B1x^3 + B2x^2 + B3x + B4$$

The complete output for one detector is given in appendix E.

TABLE 4.1

POLYNOMIAL COEFFICIENTS

	COEFFICIENTS				
DET /RANGE	*B1*	*B2*	*B3*	*B4*	*B5*
REF / 1	0.323	−2.176	8.720	−14.111	−0.020
1 / 1	0.178	−1.302	5.549	−12.556	−0.009
1 / 2	7.145	−15.181	18.276	−17.164	−1.341
2 / 1	0.433	−2.562	8.510	−15.779	−0.029
2 / 2	3.832	−10.783	16.790	−18.647	−0.525
3 / 1	0.205	−1.423	5.843	−12.975	−0.012
3 / 2	5.599	−13.747	18.486	−17.943	−0.900

4.3 POWER TRACKING

To make sure the six-port was behaving linearly, the circuit of figure 4.5 was used to track discrete input power changes. The change in power was monitored by an HP power meter at one arm of a matched power splitter. The power was changed in 1 dB steps and the power measured at the four detectors was stored. Table 4.2 shows the results of the test.

Average errors of 1.48 and 1.08 % were found for the two ranges. This represents a good tracking of power. These small errors could easily be accounted for in the

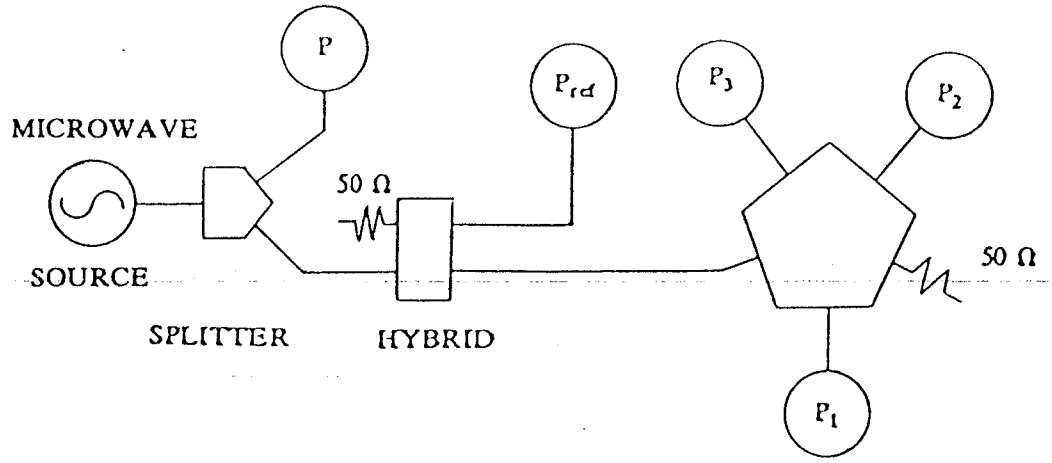

Figure 4.5: POWER TRACKING SET UP

TABLE 4.2

POWER TRACKING

POWER CHANGE AT P		*DETECTOR READINGS (dBm)*	*CHANGE IN POWER DETECTED*	*ERROR %*
1.00 *to* 0.00 *dBm*	*REF DET*	0.18 *to* −0.83	1.01	0.6
	DET 1	−5.30 *to* −6.29	0.99	1.4
	DET 2	−5.91 *to* −6.94	1.03	2.6
	DET 3	−5.26 *to* −6.27	1.01	1.3
0.00 *to* −1.00 *dBm*	*REF DET*	−0.83 *to* −1.82	0.94	0.6
	DET 1	−6.286 *to* −7.31	1.03	2.6
	DET 2	−6.286 *to* −7.95	1.01	0.7
	DET 3	−6.27 *to* −7.27	1.00	0.4

calibration procedure and would cause a maximum of 3 % error in Γ_L (as will be shown in section 5.1).

4.4 DETECTOR FLATNESS ON FREQUENCY

The detectors are said to have a flatness of ±0.5 dB over their entire range (100 kHz to 4 GHz). To check this the power versus voltage procedure was followed at 900, 950, 1000, 1050 and 1100 MHz for three of the detectors. The results shown on figures 4.6, 4.7 and 4.8 indicate excellent agreement over the band of interest. This allows us to use the same polynomials determined at 1 GHz for all frequencies from 900 to 1100 MHz.

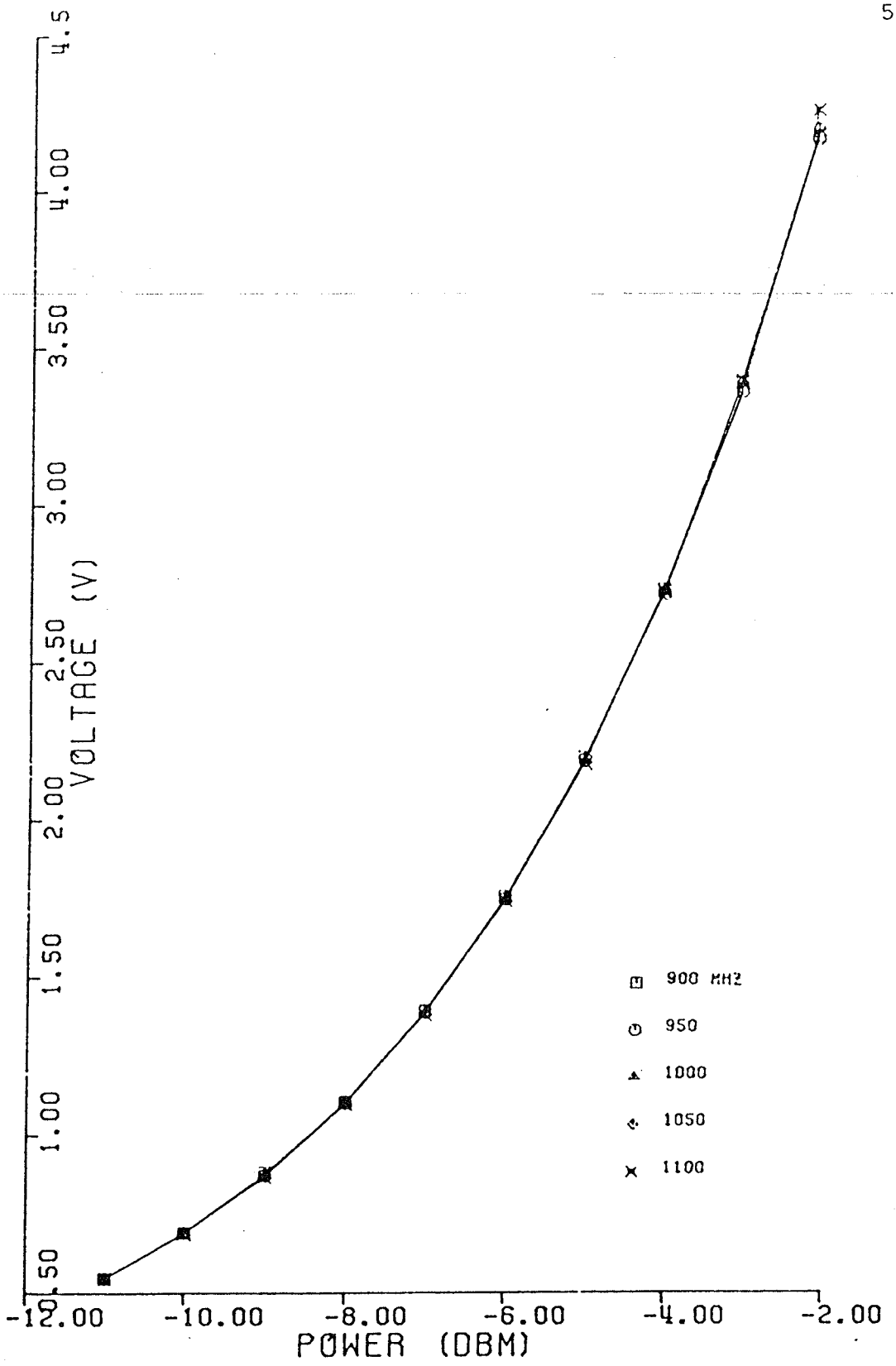

Figure 4.6: DETECTOR 1 P vs. V WITH FREQUENCY

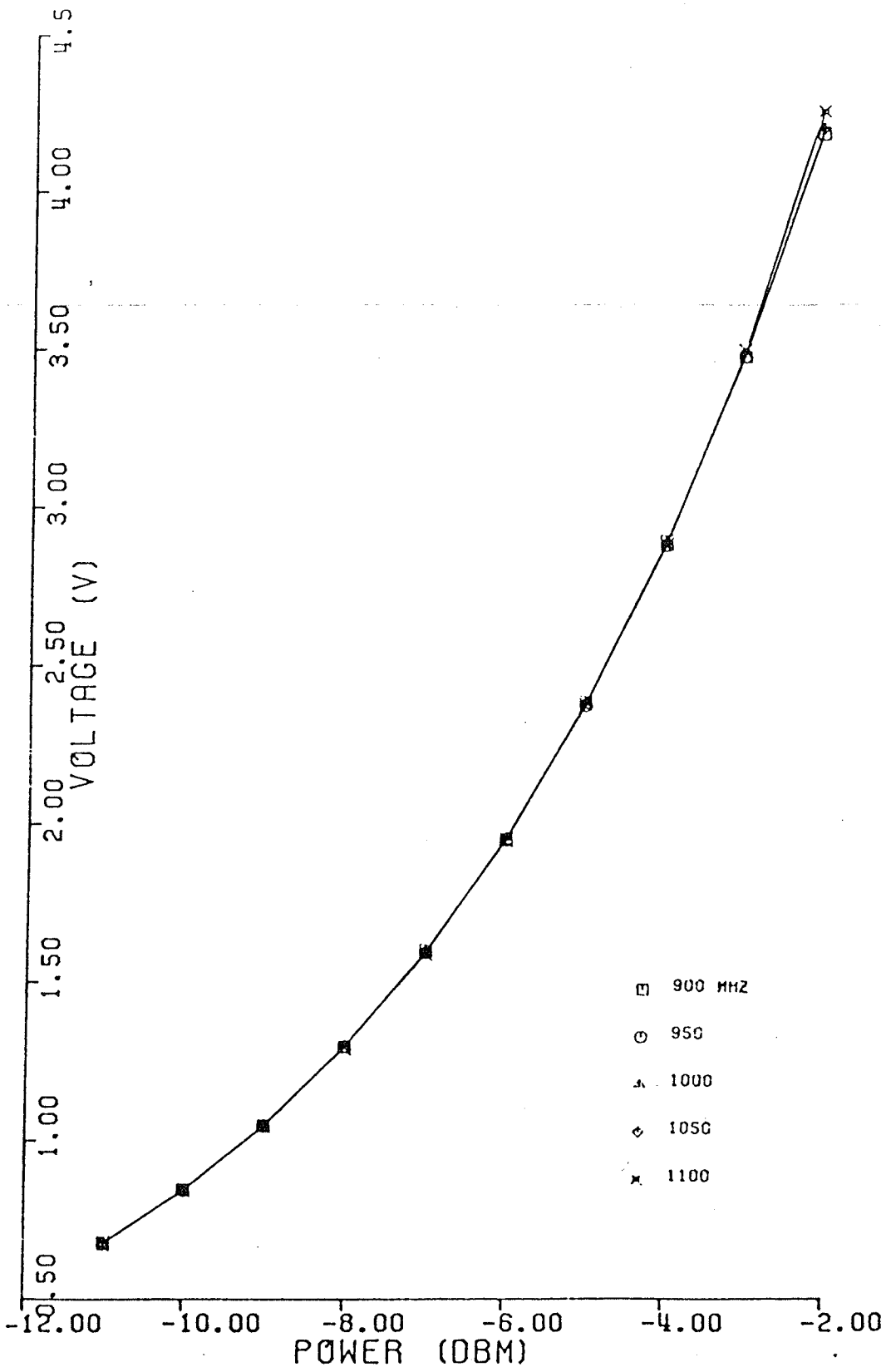

Figure 4.7: DETECTOR 2 P vs. V WITH FREQUENCY

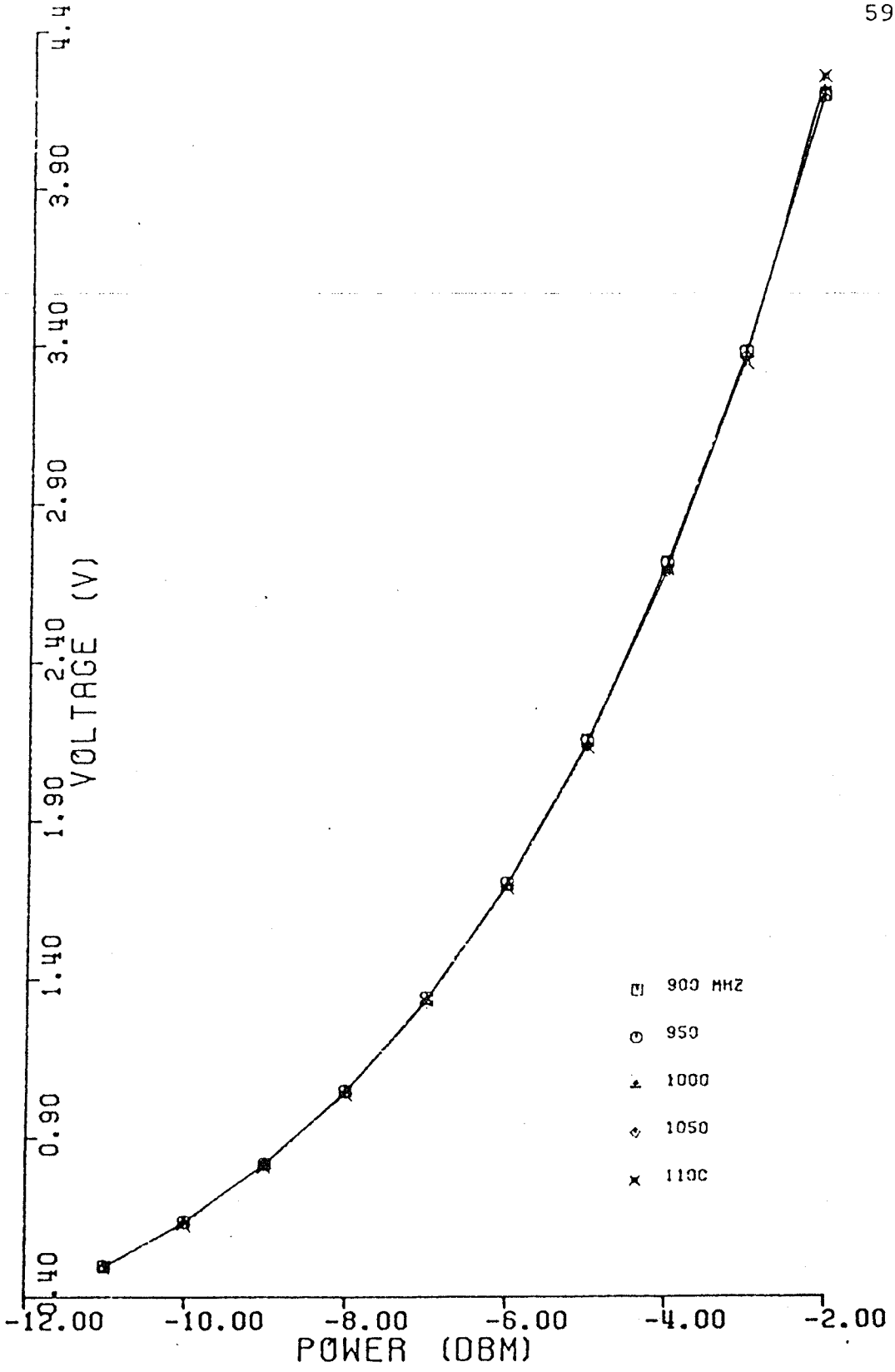

Figure 4.8: DETECTOR 3 P vs. V WITH FREQUENCY

Chapter V

EXPERIMENTATION

The experimentation performed on the six-port system is described in this chapter in three main sections. First a sensitivity study on Γ_L measurements was done with respect to the power readings. Then the calibration constants were obtained over the frequency band and their variations were observed. Finally, a series of reflection coefficient measurements were performed to evaluate the system accuracy.

5.1 SENSITIVITY

Initially a sensitivity study was done to see how errors in the power readings affect the final determination of Γ_L. To do this the calibration procedure was run in the usual manner and Γ_L was measured for a known load (one of the calibration shorts). Then errors of $\pm$ 1, $\pm$ 5 and $\pm$10 % were artificially introduced to the powers measured. For instance a 5 % error was added to P(1) and the other powers were left as measured. The results are shown in table 5.1. Errors in the reference power had the greatest effect on $|\Gamma_L|$. This is not surprising since errors in P(ref) will be passed on to all of the other power readings during normalization. The phase of Γ_L was unaffected by changes in P(ref) because

TABLE 5.1

POWER READING SENSITIVITY

DETECTOR NUMBER i	*% ERROR IN P(i)*	*FINAL* $\lvert\Gamma_L\rvert$	*FINAL* ϕ_L	*%ERROR IN* $\lvert\Gamma_L\rvert$	*%ERROR IN* ϕ_L
	0	1.007	259.75	0	0
1	1	1.027	260.05	−1.97	−0.12
	−1	0.992	259.40	1.48	0.13
	5	1.084	261.34	−7.57	−0.06
	−5	0.930	257.92	7.68	0.70
	10	1.150	262.79	−14.20	−1.20
	−10	0.845	255.85	16.10	1.52
2	1	1.019	259.25	−1.19	0.20
	−1	1.000	260.20	0.70	−0.21
	5	1.047	257.43	−3.90	0.93
	−5	0.971	262.03	3.60	−0.91
	10	1.080	255.27	−7.30	1.80
	−10	0.933	264.30	7.40	−1.82
3	1	1.016	259.80	−0.90	−0.02
	−1	1.003	259.65	0.40	0.41
	5	1.031	260.18	−2.31	−0.22
	−5	0.989	259.28	1.84	0.20
	10	1.049	260.67	−4.11	−0.43
	−10	0.970	258.84	3.73	0.40
REF	1	0.982	259.76	2.55	0.00
	−1	1.033	259.73	−2.51	0.00
	5	0.876	259.84	13.02	0.00
	−5	1.134	259.65	−12.22	0.00
	10	0.736	259.92	26.93	0.05
	−10	1.259	259.56	−25.01	0.05

all the power readings were changed by the same amount. The magnitude of Γ_L was also sensitive to errors in P(1) and P(2) but to a lesser extent to P(3). The location of these detectors around the five-port junction is most likely the reason for this since detector 1 and detector 2 straddle the test port and are more tightly coupled to it than detector 3 which is almost opposite in junction location.

With the detectors at the stabilized temperature and the fourth order polynomial approximations applied, detectors 1, 2 and 3 agreed with digital power meter readings to within 5%. The reference detector readings were within 1% because its range was smaller and its detected power was higher. If we consider a worst case of 5% error in power readings at detectors 1, 2 and 3 and a 1% error in the reference power, we can add the errors found in table 5.1, since the six-port is a linear device, and find a total error of about 16% in magnitude and about 1% in phase of Γ_L .

5.2 CALIBRATION CONSTANTS VERSUS FREQUENCY

The six-port was calibrated at 900, 950, 1000, 1050 and 1100 MHz to see how the six-port constants vary with frequency. The figure 5.1 shows a polar display of the constants. The constants X1, X2 and X3 were found to vary smoothly over the band. This is a positive result because the six-port could be calibrated at discrete frequencies (as was done here) and values for any intermediate frequencies

could be approximated by interpolation. Although Z and ϕ_Z do not vary as smoothly, one could still determine intermediate values by characterizing Z and ϕ_Z as was done for the detectors.

We can see from figure 5.1 that Z very nearly passes through Z=0, the ideal value. By running the calibration procedure at several frequencies between 950 and 1000 MHz, it was found that 980 MHz was as close as the system would come to ideal. The constants at this frequency were: Z = $0.019 \angle 19.8^\circ$, X1 = $0.521 \angle 82.1^\circ$, X2 = $0.485 \angle -162.2^\circ$ and X3 = $0.444 \angle -39.4^\circ$. The X values are close to the ideal value of 0.5 (given in [5]). The phase differences between them are 116°, 123°, and 121° which are also close to the ideal 120° separation. A matched 50 Ω load was measured using these constants and was found to have a magnitude $|\Gamma_L| = 0.07$, which is close to a perfect match. A short circuited 3 dB attenuator was also measured using these constants and the results were compared to calculated values. The magnitude was within 0.5 % and the phase was within 1.6 % of the calculated values.

It is interesting to note that the six-port constants found here agree closely to the ones found by Girimaji [11] for the same five-port ring structure (see appendix G for his results).

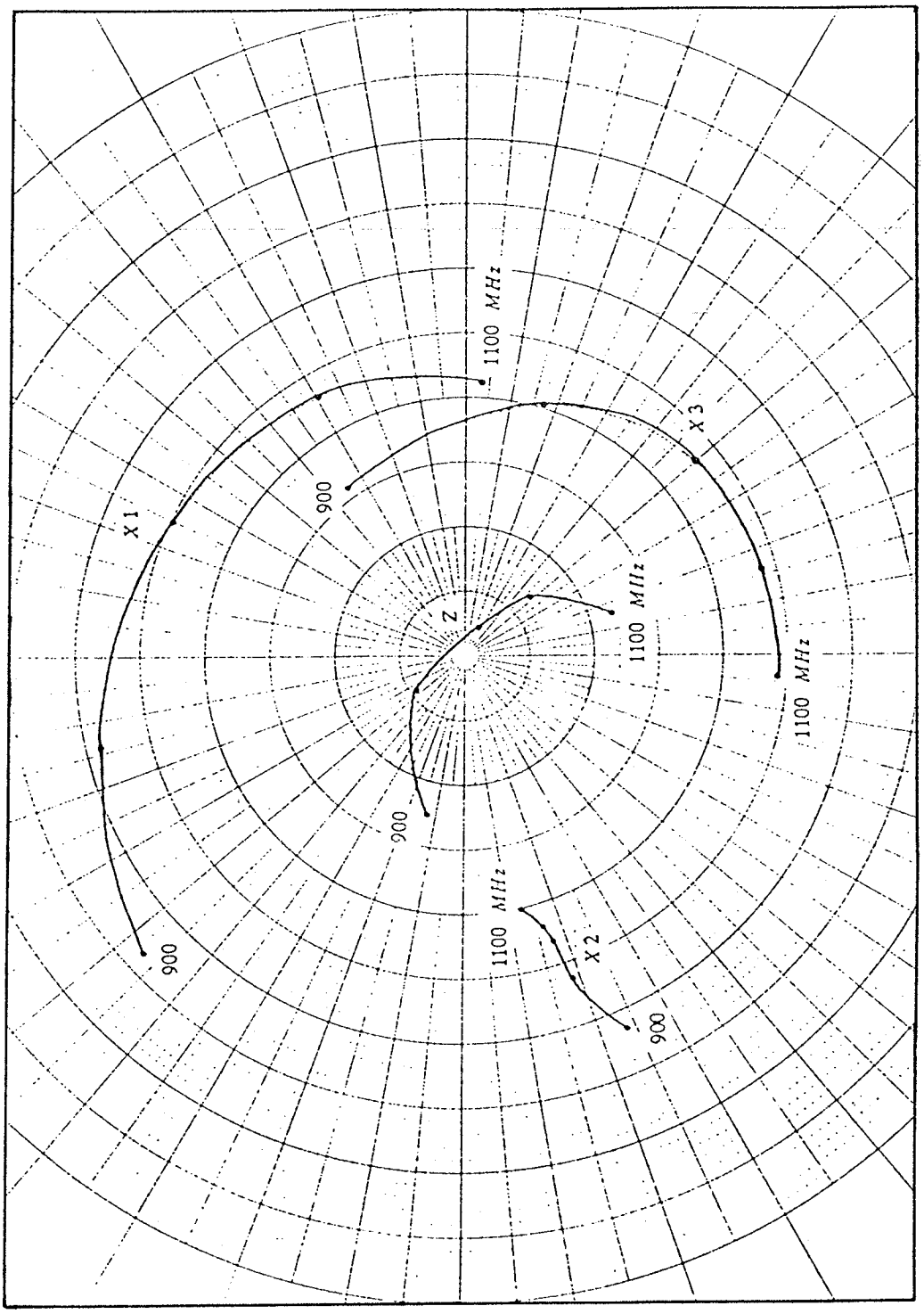

Figure 5.1: Polar Display of Six-Port Constants

5.2.1 Trial Γ_L Measurements

The first and simplest trial measurements of Γ_L are those made on the calibration standards themselves. Accurate slotted line measurements are available for comparison. The Smith Chart of figure 5.2 shows the results of such a comparison. The agreement at 1 GHz for all loads was within 0.3 % in phase and better than 1 % in magnitude. At 1100 MHz the error in magnitude of one of the standards, short 0, was about 9 % but the phase was almost exact (less than 1° error). At 1050 MHz this same standard had an error in magnitude of about 4 % and was near exact in phase when compared to slotted line measurements. At the other measured frequencies, this standard had less than 1 % error in magnitude and less than 1° error in phase. The measurements for the other standards were also within 1 % in magnitude and 1° in phase for all tested frequencies.

A short circuited 3 dB attenuator was used as a reflection coefficient standard (ideally $|\Gamma_L| = 0.5$). Measurements were taken for the entire frequency range in 50 MHz steps and the results were compared to ANA measurements, see table 5.2. Here again the largest magnitude error,16.5 %, was found at 1100 MHz. At this frequency the phase error was 7.8 %. The smallest magnitude error, 1.45 %, was found at 900 MHz, where the phase error was 1.33 %.

TABLE 5.2

3 dB ATTENUATOR RESULTS

FREQUENCY	*NETWORK ANALYZER*		*SIXPORT*		% *ERROR*	% *ERROR*
	$\lvert\Gamma_L\rvert$	ϕ_L	$\lvert\Gamma_L\rvert$	ϕ_L	$\lvert\Gamma_L\rvert$	ϕ_L
900	0.550	97.5	0.558	98.8	−1.45	−1.33
950	0.555	95.5	0.566	94.7	−1.98	0.84
1000	0.560	93.0	0.569	90.0	−1.61	3.23
1050	0.570	90.0	0.540	84.2	5.26	6.44
1100	0.575	87.0	0.480	80.2	16.5	7.82

Next a matched load was measured in the same frequency range and interval. The magnitude of the reflection coefficient was found to be less than 0.1 for all frequencies while the phases varied considerably as expected. When the reflection coefficient for the same matched load was measured on the ANA, with the reference plane set at 1 GHz, the same general phase distribution was observed.

As a final test load element, a coaxial T junction was terminated at two of its junctions in sliding shorts. An ANA was used to adjust the short lengths such that an over coupled resonant circuit was formed. The results of Γ_L measurements over a 1000 MHz to 1100 MHz range with both the

ANA and the six-port are shown on the Smith chart of figure 5.3. Magnitude errors from 1.1 to 10.3 % were found and the phase errors ranged from 1.4 to 12.5 %. These errors are not as bad as they seem when figure 5.3 is studied. The rapid change of impedance with frequency shows that the resonant circuit has a very high Q. Because the sliding shorts were not fixed, errors in the magnitude and phase could have been introduced by small movements of the stub lengths when the T junction was moved from the ANA to the six-port system. The reference planes of the two measurement systems may also differ enough to change the resonant frequency of such a high Q circuit. The six-port measurements did follow the basic shape of the resonant path.

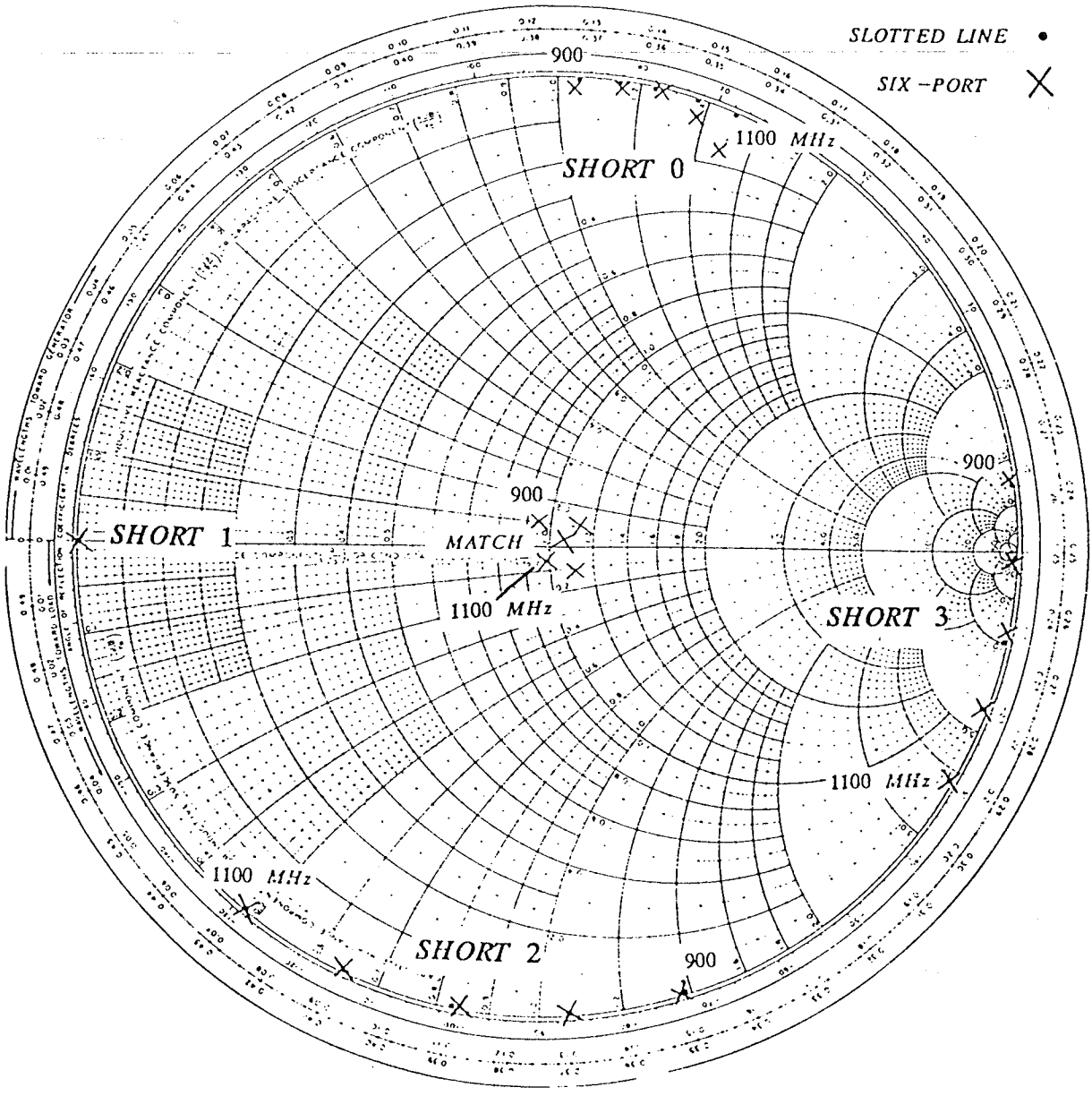

Figure 5.2: REFLECTION COEFFICIENT MEASUREMENT

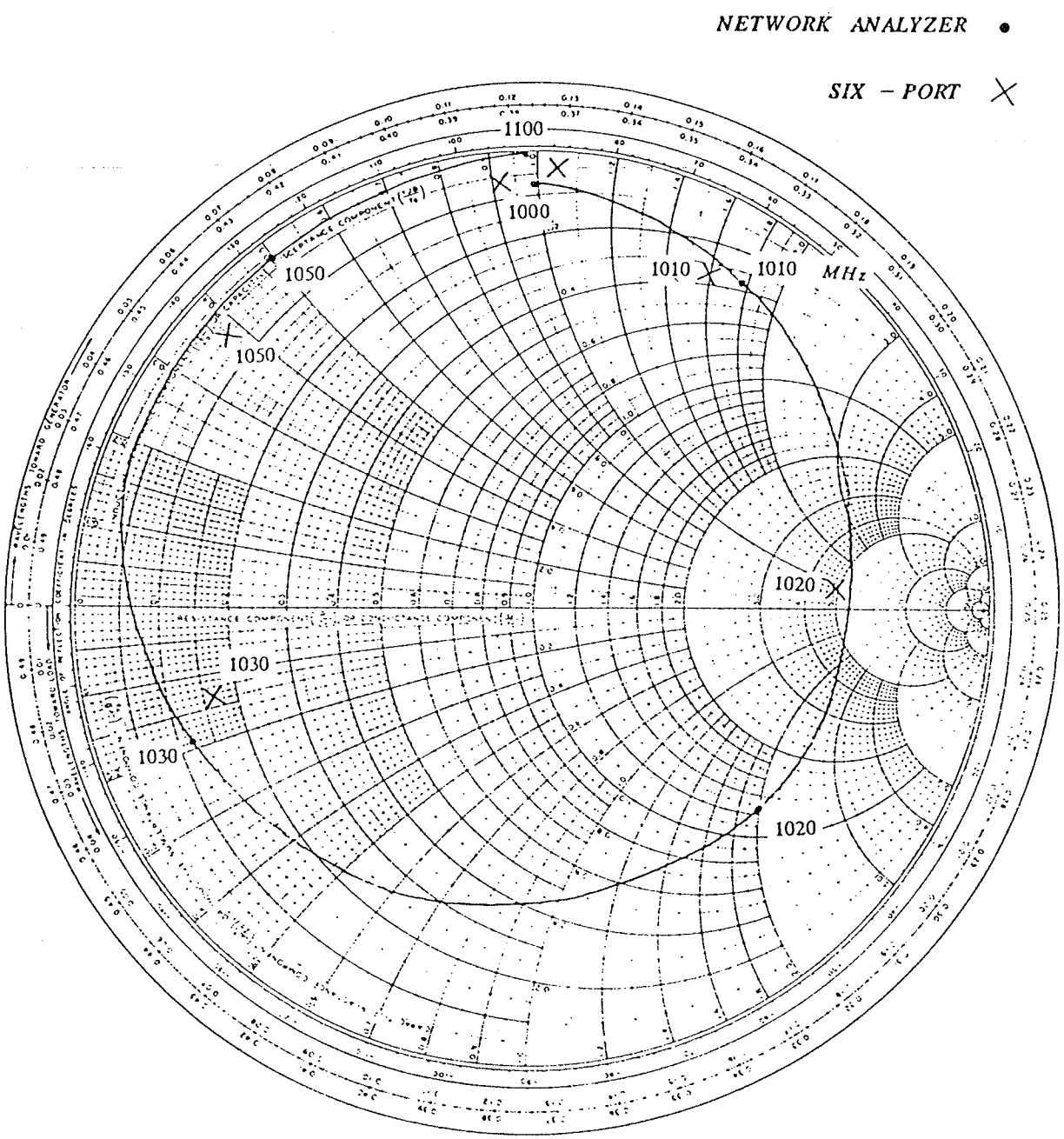

Figure 5.3: RESONANT CIRCUIT MEASUREMENTS

Chapter VI

CONCLUSIONS

In this paper a six-port microwave measurement system was developed to measure the complex reflection coefficient of a terminating microwave device from power measurements at four of the six ports. Before the six-port can be used to measure reflection coefficients seven calibration constants must be determined for each frequency, using a new calibration procedure [3], which relate the power at the four detector ports to the reflection coefficient of a device terminating the test port.

The six-port consists of a symmetrical five-port power divider, a 90° hybrid junction and four diode amplitude detectors. The five-port power divider operated well at 1 GHz, the center of a 200 MHz frequency band. However, closer to the band edges, the performance was less than ideal. The new calibration procedure was implemented to minimize the effects of these system imperfections and errors in the power detection scheme. The six-port constants determined using this calibration procedure were close to the ideal values given by other investigators [5] at the center frequency.

Power detection at the four ports is accomplished by measuring the output dc voltage of a detector and applying it to a fourth order polynomial approximation which models the detector's input RF power versus output dc voltage curve. An HP 85 desktop computer obtains a digital value of these dc voltages from an A/D converter through an interface bus. The electrical characteristics of the diode detectors are stabilized by placing them in a temperature controlled oven. The temperature of the oven was held at 35 $\pm$0.5 C by a temperature control circuit developed in this thesis. With the fourth order polynomial approximations applied and the temperature stabilized, the power measurement of the three detectors on the five-port had an average error of 5% when compared to digital power meter readings. The reference detector had an average error of about 1%.

To test the six-port system, the reflection coefficients of several loads were measured and the results were compared to slotted line and automatic network analyzer (ANA) measurements. First, the calibration standards were measured for the 200 MHz frequency band in 50 MHz steps. The results showed agreement to within 4% in magnitude and within 1% in phase when compared to slotted line measurements for all frequencies but 1100 MHz. At this frequency the error in magnitude was 9% but the phase was within 1%. A short circuited 3 dB attenuator was also used as a test load over the band and the six-port results were

compared to ANA measurements. Again the largest error, 16.5%, was found at 1100 MHz where the phase error was 7.8%. At 900 MHz the error in both magnitude and phase were within 1.5% A matched load was also measured, with a reflection coefficient magnitude of less than 0.1 for all frequencies. Finally, a high Q resonant circuit was measured over the upper half of the frequency band. The six-port results followed the pattern of the resonant path as measured on an ANA, though errors in magnitude of 1 to 10% and errors in phase of 1 to 12% were found.

In conclusion, the six-port system developed in this thesis worked very well for most of the band of interest and the computer control of the calibration procedure and reflection coefficient measurements make it as simple to operate as an automated network analyzer. The new calibration procedure produced good results and errors in power measurement and system imperfections were minimized for most of the band. The new calibration procedure can be extended for use with other six-port systems which use the symmetric five-port ring structure. For instance, the dimensions of the five-port could be changed to measure reflection coefficients in a different band of frequencies.

Future considerations would include automatic frequency control to enable the user to calibrate and use the six-port system over the entire frequency band at once. If a programable source were used, power measurements could be

taken for the band of frequencies in certain intervals for each calibration standard. This would save the time of connecting and disconnecting the five standards for each frequency. Then, once the calibration constants were determined on these intervals, they would be stored in computer memory. In measuring reflection coefficients, one would enter the measurement frequencies, connect the load device, and start the data acquisition. Power readings would be taken at all frequencies of interest and the calibration constants would be called from memory or calculated from the stored values by an interpolation routine. The reflection coefficient would then be calculated for all frequencies entered.

REFERENCES

[1] G.F. Engen , "An Improved Circuit for Implementing the Six-Port Technique of Microwave Measurements", IEEE Trans. vol. MTT-25, No. 12, pp. 1080-1083, 1977.

[2] G.F. Engen and C.A. Hoer, "Application of an Arbitrary Six-Port Junction to Power-Measurement Problems", IEEE Trans. vol. IM-21, pp. 470-474, Nov. 1972.

[3] J. Dobrowolski, E. Bridges and L. Shafai, "A Calibration Procedure for a Single Six-Port Reflectometer by Means of a Load and Offset Reflection Standards", Department of Electrical Engineering, The University of Manitoba, Winnipeg, June 1984.

[4] G.F. Engen, "The Six-Port Reflectometer: An Alternative Network Analyzer", IEEE Trans. vol. MTT-25, No. 12, pp. 1075-1079 Dec. 1977.

[5] E.R.B. Hansson and G.P. Riblet, "An Ideal Six-Port Network Consisting of a Matched Reciprocal Lossless Five-Port and a Perfect Directional Coupler", IEEE Trans. vol. MTT-31, No. 3, pp. 284-288, Mar. 1983.

[6] G.P. Riblet and E.R.B. Hansson, "Aspects of the Calibration of a Single Six-Port using a load and offset reflection standards", IEEE Trans. vol. MTT-30, No. 12, pp. 2120-2125, Dec. 1982.

[7] A.L. Cullen, S.K. Judah and F. Nikravesh, "Impedance Measurement Using a Six-Port Directional Coupler", IEE Proc. vol. 127, H, No.2, pp. 92-97, April 1980.

[8] H.M. Cronson and L. Susman, "A Six-Port Automatic Network Analyzer", IEEE Trans. vol. MTT-25, No. 12, pp. 1086-1091, Dec. 1977

[9] D. Woods, "Analysis and Calibration theory of the General Six-Port Reflectometer Employing Four Amplitude Detectors", IEEE Proc. vol. 126, No. 2, pp.221-228, Feb. 1979.

[10] R.H. Dicke, C.G. Montgomery and E.M. Purcell, "Principles of Microwave Circuits". New York : McGraw - Hill, 1948.

[11] J. Girimaji, "Development of a Computer Controlled Six-Port Microwave Measurement System", University of Manitoba Masters Thesis, 1983

[12] J.F. Traub, "Iterative Methods for the Solution of Equations", Englewood Cliffs, N. Y. : Prentice - Hall Inc., 1964.

Appendix A

SOLUTION OF THE MATRIX:

$$\begin{bmatrix} R_{1i} & R_{1i}\cos\phi_1 & -R_{1i}\sin\phi_1 \\ R_{2i} & R_{2i}\cos\phi_2 & -R_{2i}\sin\phi_2 \\ R_{3i} & R_{3i}\cos\phi_3 & -R_{3i}\sin\phi_3 \end{bmatrix} \begin{bmatrix} 1+Z^2 \\ 2Z\cos\phi_Z \\ 2Z\sin\phi_Z \end{bmatrix} = \begin{bmatrix} 1 & \cos\phi_1 & -\sin\phi_1 \\ 1 & \cos\phi_2 & -\sin\phi_2 \\ 1 & \cos\phi_3 & -\sin\phi_3 \end{bmatrix} \begin{bmatrix} 1+X_i^2 \\ 2X_i\cos\phi_{xi} \\ 2X_i\sin\phi_{xi} \end{bmatrix} \quad (A.1)$$

and

$$R_{0i}(1+Z^2) + R_{0i}\cos\phi_0 2Z\cos\phi_Z - R_{0i}\sin\phi_0 2Z\sin\phi_Z = 1 + X^{2_i} + \cos\phi_0 \cdot 2X_i\cos\phi_{xi} - \sin\phi_0\, 2X_i\sin\phi_{xi} \quad (A.2)$$

Letting

$$\begin{bmatrix} 1+X_i^2 \\ 2X\cos\phi_{xi} \\ 2X\sin\phi_{xi} \end{bmatrix} = [B]\cdot\begin{bmatrix} 1+Z^2 \\ 2Z\cos\phi_Z \\ 2Z\sin\phi_Z \end{bmatrix} \quad (A.3)$$

where

$$[B] = \frac{1}{\sin(\phi_1-\phi_2)+\sin(\phi_2-\phi_3)+\sin(\phi_3-\phi_1)} \cdot \begin{bmatrix} \sin(\phi_2-\phi_3) & \sin(\phi_3-\phi_1) & \sin(\phi_1-\phi_2) \\ \sin\phi_3-\sin\phi_2 & \sin\phi_1-\sin\phi_3 & \sin\phi_2-\sin\phi_1 \\ \cos\phi_3-\cos\phi_2 & \cos\phi_1-\cos\phi_3 & \cos\phi_2-\cos\phi_1 \end{bmatrix} \cdot \begin{bmatrix} R_{1i} & R_{1i}\cos\phi_1 & -R_{1i}\sin\phi_1 \\ R_{2i} & R_{2i}\cos\phi_2 & -R_{2i}\sin\phi_2 \\ R_{3i} & R_{3i}\cos\phi_3 & -R_{31}\sin\phi_3 \end{bmatrix}$$

Substituting (A.3) into (A.2) we have three equations in the quantities

$1 + Z^2$, $Z\cos\phi_Z$ and $Z\sin\phi_Z$

We can write these equations in matrix form as :

$$[A] \cdot \begin{bmatrix} 1 + Z^2 \\ 2Z\cos\phi_Z \\ 2Z\sin\phi_Z \end{bmatrix} = 0 \qquad \text{(A.4)}$$

Where the elements of $[A]$ *are found from :*

$$\begin{bmatrix} R_{1i} - R_{0i} & R_{2i} - R_{0i} & R_{3i} - R_{0i} \\ R_{1i}\cos\phi_1 - R_{0i} & R_{2i}\cos\phi_2 - R_{0i} & R_{3i}\cos\phi_3 - R_{0i} \\ -R_{1i}\sin\phi_1 & -R_{2i}\sin\phi_2 & -R_{3i}\sin\phi_3 \end{bmatrix}$$

$$\cdot \begin{bmatrix} \sin\phi_2 - \sin\phi_3 - \sin(\phi_2 - \phi_3) \\ \sin\phi_2 - \sin\phi_1 - \sin(\phi_3 - \phi_1) \\ \sin\phi_1 - \sin\phi_2 - \sin(\phi_1 - \phi_2) \end{bmatrix} \begin{bmatrix} 1 + Z^2 \\ 2Z\cos\phi_Z \\ 2Z\sin\phi_Z \end{bmatrix} = \begin{bmatrix} A_{i1} \\ A_{i2} \\ A_{i3} \end{bmatrix} \qquad i = 1,2,3$$

From (A.4) we can write

$$A_{11}(Z + 1/Z)/2 + A_{12}\cos\phi_Z + A_{13}\sin\phi_Z = 0$$

$$A_{21}(Z + 1/Z)/2 + A_{22}\cos\phi_Z + A_{23}\sin\phi_Z = 0$$

$$A_{31}(Z + 1/Z)/2 + A_{32}\cos\phi_Z + A_{33}\sin\phi_Z = 0$$

Appendix B

MATRIX MANIPULATION OF EQUATION

$$\underline{A}\underline{z} + \underline{c} = [\underline{B}^{-1}(\underline{A}_1\underline{z} + \underline{c}_1) \quad \underline{B}^{-1}(\underline{A}_2\underline{z} + \underline{c}_2) \quad \underline{B}^{-1}(\underline{A}_3\underline{z} + \underline{c}_3)]^T \underline{b}_0$$

$$= (\underline{B}^{-1}[\underline{A}_1\underline{z} + \underline{c}_1 \quad \underline{A}_2\underline{z} + \underline{c}_2 \quad \underline{A}_3\underline{z} + \underline{c}_3])^T \underline{b}_0$$

$$= [\underline{A}_1\underline{z} + \underline{c}_1 \quad \underline{A}_2\underline{z} + \underline{c}_2 \quad \underline{A}_3\underline{z} + \underline{c}_3]^T (\underline{B}^{-1})^T \underline{b}_0$$

$$= ([\underline{A}_1\underline{z} \quad \underline{A}_2\underline{z} \quad \underline{A}_3\underline{z}] + [\underline{c}_1 \quad \underline{c}_2 \quad \underline{c}_3])^T (\underline{B}^{-1})^T \underline{b}_0$$

$$= [\underline{A}_1\underline{z} \quad \underline{A}_2\underline{z} \quad \underline{A}_3\underline{z}]^T (\underline{B}^{-1})^T \underline{b}_0 + [\underline{c}_1 \quad \underline{c}_2 \quad \underline{c}_3]^T (\underline{B}^{-1})^T \underline{b}_0$$

Appendix C

RESULTS OF DETECTOR RANGE DETERMINATION

LOAD REF.COEF. MAG.	PHASE(deg)	P1/Pref	P2/Pref	P3/Pref
1.00	0.0	.398	.065	.437
1.00	10.0	354	.080	.463
1.00	20.0	.310	.101	.483
1.00	30.0	.268	.126	.498
1.00	40.0	.229	.156	.506
1.00	50.0	.193	.189	.509
1.00	60.0	.162	.224	.507
1.00	70.0	.135	.260	.499
1.00	80.0	.114	.297	.485
1.00	90.0	.099	.333	.467
1.00	100.0	.089	.369	.445
1.00	110.0	.086	.402	.418
1.00	120.0	.090	.433	.389
1.00	130.0	.100	.460	.356
1.00	140.0	.116	.483	.322
1.00	150.0	.139	.501	.287
1.00	160.0	.167	.514	.251
1.00	170.0	.201	.520	.215
1.00	180.0	.239	.520	.182
1.00	190.0	.281	.513	.151
1.00	200.0	.326	.499	124
1.00	210.0	.373	.478	.101
1.00	220.0	.419	.450	.085
1.00	230.0	.463	.416	.075
1.00	240.0	.504	.377	.083
1.00	250.0	.539	.335	.079
1.00	260.0	.567	.290	.093
1.00	270.0	.587	.246	.114
1.00	280.0	.590	.203	.142
1.00	290.0	.600	.163	.175
1.00	300.0	.592	.128	.212
1.00	310.0	.575	.099	.252
1.00	320.0	.550	.077	.293
1.00	330.0	.519	.062	.333
1.00	340.0	.482	.056	.371
1.00	350.0	.441	.097	.406
1.00		.398	.065	.437

Appendix D

DETECTOR POWER VERSUS VOLTAGE DATA

DETECTOR / RANGE	*VOLTAGE*	*POWER (dBm)*
1 / 1	4.90	−1.3
	4.25	−2
	3.43	−3
	2.75	−4
	2.19	−5
	1.74	−6
1 / 2	1.74	−6
	1.37	−7
	1.07	−8
	0.83	−9
	0.35	−10
	0.50	−11
2 / 1	4.67	−1.5
	4.28	−2
	3.58	−3
	2.97	−4
	2.44	−5
	2.00	−6
	1.64	−7

DETECTOR / RANGE	*VOLTAGE*	*POWER (dBm)*
2 / 2	1.64	−7
	1.34	−8
	1.08	−9
	0.86	−10
	0.70	−11
	0.56	−12
	0.45	−13
3 / 1	4.75	−1.5
	4.29	−2
	3.49	−3
	2.80	−4
	2.25	−5
	1.80	−6
3 / 2	1.80	−6
	1.43	−7
	1.13	−8
	0.89	−9
	0.71	−10
	0.56	−11
REF / 1	4.98	3.2
	4.34	2.2
	3.77	1.2
	3.27	0.2
	2.83	−0.8
	2.44	−1.8
	2.09	−2.8
	1.79	−3.8
	1.53	−4.8
	1.30	−5.8

```
1       S A S   L O G    OS SAS 82.4        VS2/MVS JOB WOODSS   STEP GO       PROC

NOTE: THE JOB WOODS$ HAS BEEN RUN UNDER RELEASE 82.4 OF SAS AT THE UNIVERSITY OF MANITOBA

NOTE: CPUID   VERSION = 96  SERIAL = 000103  MODEL = 0580 .

NOTE: SAS OPTIONS SPECIFIED ARE:
      S=80 SORT=4

1           TITLE POLYNOMIAL:Y=B5*X**4+B1*X**3+B2*X**2+B3*X+B4;
2           DATA A;
3            INPUT X Y @@;
4            PUT X Y ;
5            CARDS;

4.98 3.2
4.34 2.2
3.772 1.2
3.272 0.2
2.828 -0.8
2.441 -1.8
2.094 -2.8
1.796 -3.8
1.532 -4.8
1.301 -5.8
NOTE: SAS WENT TO A NEW LINE WHEN INPUT STATEMENT
      REACHED PAST THE END OF A LINE.
NOTE: DATA SET WORK.A HAS 10 OBSERVATIONS AND 2 VARIABLES. 953 OBS/TRK.
NOTE: THE DATA STATEMENT USED 0.04 SECONDS AND 332K.

8           ;
9           PROC NLIN BEST=1 PLOT METHOD=GAUSS CONVERGENCE=0.0000000001;
10          PARMS B1=40.00 B2=-50.00 B3=40.0 B4=-20.000 B5=-10.0000  ;
11           MODEL Y=B5*X**4+B1*X**3+B2*X**2+B3*X+B4;
12           DER.B5=X**4;
13           DER.B1=X**3;
14           DER.B2=X**2;
15           DER.B3=X;
16           DER.B4=1;
17           OUTPUT OUT=B P=YHAT R=YRESID;

NOTE: DATA SET WORK.B HAS 10 OBSERVATIONS AND 4 VARIABLES. 529 OBS/TRK.
NOTE: THE PROCEDURE NLIN USED 0.13 SECONDS AND 422K AND PRINTED PAGES 1 TO 2.

18          PROC PLOT DATA=B;
19           PLOT Y*X='A' YHAT*X='P'/OVERLAY VPOS=25;
20           PLOT YRESID*X/VREF=0 VPOS=25;

NOTE: THE PROCEDURE PLOT USED 0.10 SECONDS AND 390K AND PRINTED PAGES 3 TO 4.
NOTE: SAS USED 422K MEMORY.

NOTE: SAS INSTITUTE INC.
      SAS CIRCLE
      PO BOX 8000
      CARY, N.C.  27511-8000
```

NON-LINEAR LEAST SQUARES ITERATIVE PHASE

DEPENDENT VARIABLE: Y METHOD: GAUSS-NEWTON

ITERATION	B1	B2	B3	B4	B5	RESIDUAL SS
0	40.00000000	-50.00000000	40.00000000	-20.00000000	-10.00000000	6557064.06490077
1	0.32342667	-2.17641448	8.71962299	-14.11138986	-0.01964561	0.00032198
2	0.32342664	-2.17641437	8.71962279	-14.11138973	-0.01964561	0.00032198

NOTE: CONVERGENCE CRITERION MET.

POLYNOMIAL:Y=B5*X**4+B1*X**3+B2*X**2+B3*X+B4 18:10 FRIDAY, JULY 26, 1985

NON-LINEAR LEAST SQUARES SUMMARY STATISTICS DEPENDENT VARIABLE Y

SOURCE	DF	SUM OF SQUARES	MEAN SQUARE
REGRESSION	5	99.39967802	19.87993560
RESIDUAL	5	0.00032198	0.00006440
UNCORRECTED TOTAL	10	99.40000000	
(CORRECTED TOTAL)	9	82.50000000	

PARAMETER	ESTIMATE	ASYMPTOTIC STD. ERROR	ASYMPTOTIC 95 % CONFIDENCE INTERVAL LOWER	UPPER
B1	0.32342664	0.02918342	0.24840936	0.39844392
B2	-2.17641437	0.12971798	-2.50986023	-1.84296852
B3	8.71962279	0.24080896	8.10061261	9.33863297
B4	-14.11138973	0.15638358	-14.51338070	-13.70939876
B5	-0.01964561	0.00233175	-0.02563948	-0.01365174

ASYMPTOTIC CORRELATION MATRIX OF THE PARAMETERS

	B1	B2	B3	B4	B5
B1	1.000000	-0.996538	0.984712	-0.963536	-0.997313
B2	-0.996538	1.000000	-0.995666	0.981612	0.987886
B3	0.984712	-0.995666	1.000000	-0.994852	-0.969939
B4	-0.963536	0.981612	-0.994852	1.000000	0.943272
B5	-0.997313	0.987886	-0.969939	0.943272	1.000000

POLYNOMIAL:Y=B5*X**4+B1*X**3+B2*X**2+B3*X+B4 18:10 FRIDAY, JULY 26, 1985 3

PLOT OF Y*X SYMBOL USED IS A
PLOT OF YHAT*X SYMBOL USED IS P

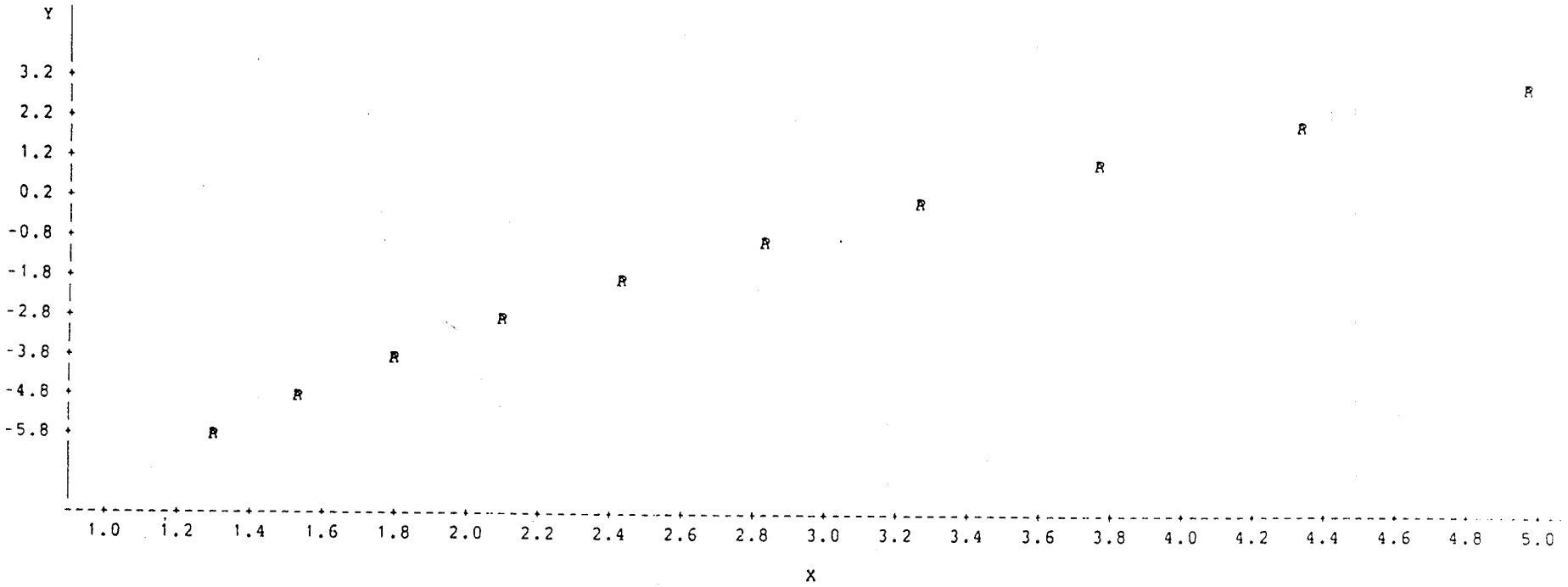

POLYNOMIAL:Y=B5*X**4+B1*X**3+B2*X**2+B3*X+B4 18:10 FRIDAY, JULY 26, 1985 4

PLOT OF YRESID*X LEGEND: A = 1 OBS, B = 2 OBS, ETC.

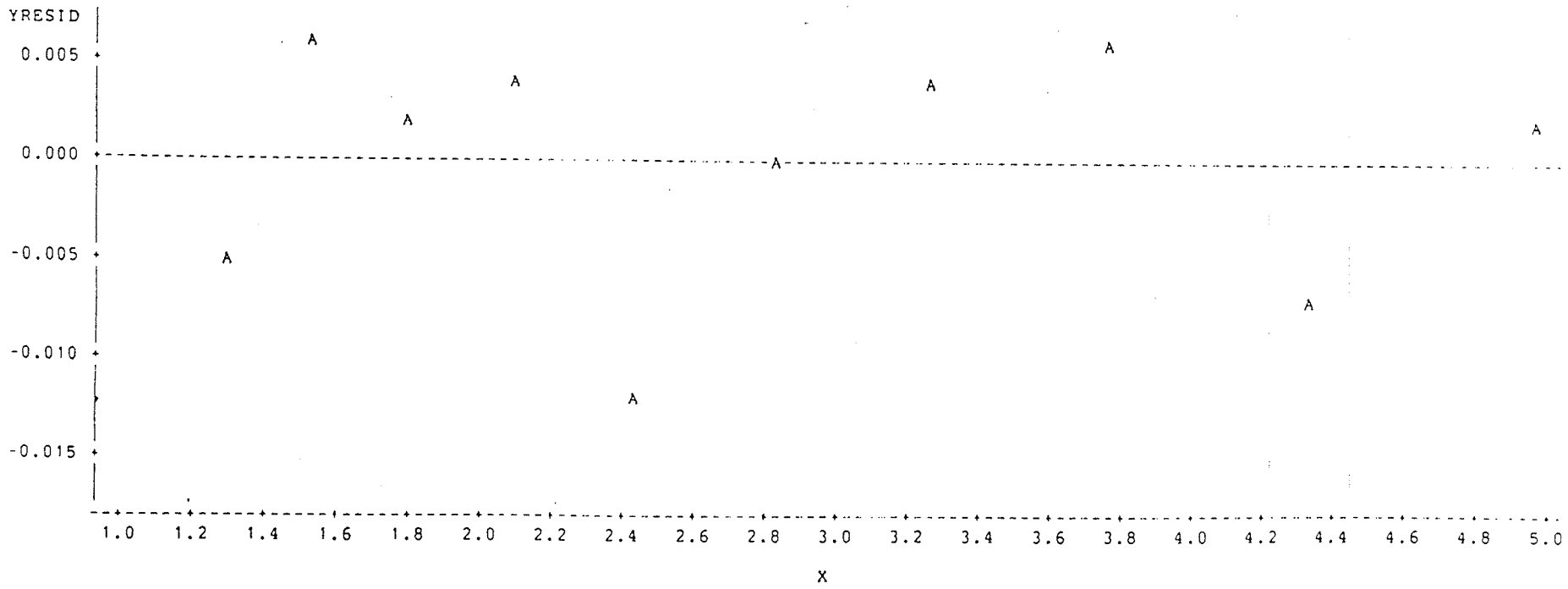

Appendix F

PROGRAM LISTINGS

GAMMA

```
210 DISP "MEASUREMENT OF REF.COE
    FF.USING  6-PORT NW!"
250 DISP
290 DISP "ENTER DATE&TRIAL #"
330 DISP
370 INPUT R$,V7
410 PRINT USING 450 ; R$,V7
450 IMAGE "OBTN6",8X,6A,6X,DDDD
490 PRINT "-------------------
    ----------"
530 PRINT
570 CLEAR
610 OPTION BASE 1
650 RAD
690 DIM F0(10),X(3),C(3,3),H(3,3
    ),P(3),B(3),P0(3),G6(3)
730 DISP "FREQUENCY SET?"
770 BEEP
810 DISP
850 INPUT E$
890 ASSIGN# 1 TO "6DATA.WDDDS"
930 READ# 1 ; B(1),B(2),B(3),Z1,
    P0(1),P0(2),P0(3),Z,X(1),X(2
    ),X(3)
970 ASSIGN# 1 TO *
1010 PRINT B(1)
1050 PRINT
1090 DISP "ENTER ESTIMATE"
1130 INPUT T$
1135 RAD
1170 DISP
1210 PRINT
1250 PRINT "++++++++++++++++++++
     ++++++++++++"
1290 PRINT USING 1330 ; T$
1330 IMAGE 20X,10A
1370 CLEAR 7
1410 V(1)=0
1450 V(2)=0
1490 V(3)=0
1530 V(4)=0
1600 FOR I=1 TO 10
1610 OUTPUT 706 USING "#,K,K" ;
     "H",1,"AJ","F"
1620 WAIT 300
1630 ENTER 706 USING "#,W" ; S
1640 V(1)=V(1)+S/2044
1650 OUTPUT 706 USING "#,K,K" ;
     "H",2,"AJ","F"
1660 WAIT 300
1670 ENTER 706 USING "#,W" , S
1680 V(2)=V(2)+S/2044
1690 OUTPUT 706 USING "#,K,K" ,
     "H",4,"AJ","F"
```

```
1700 WAIT 300
1710 ENTER 706 USING "#,W" ; S
1720 V(3)=V(3)+S/2044
1730 OUTPUT 706 USING "#,K,K" ;
     "H",8,"AJ","F"
1740 WAIT 300
1750 ENTER 706 USING "#,W" ; S
1760 V(4)=V(4)+S/2044
1770 NEXT I
1780 OUTPUT 706 USING "#,K" ; "H
     "
1790 X=V(1)
1795 H$="ONE"
1800 IF X>4.9 OR X<.3 THEN 5930
1810 IF X<1.297 THEN 1840
1820 P(1)=-.01491633*X^4+.240982
     42*X^3-1.5731517*X^2+6.036
     89409*X-12.68435425
1830 GOTO 1850
1840 P(1)=-.32255049*X^4+4.84333
     171*X^3-13.99801255*X^2+18.
     53171147*X-17.16251206
1850 X=V(2)
1855 H$="REF"
1860 IF X>4.98 OR X<1.3 THEN 593
     0
1870 R=-.01964561*X^4+.32342664*
     X^3-2.17641437*X^2+8.719622
     79*X-14.11138973
1890 X=V(3)
1895 H$="THREE"
1900 IF X>4.75 OR X<.561 THEN 59
     30
1910 IF X<1.8 THEN 1940
1920 P(3)=-.0120374*X^4+.2048173
     4*X^3-1.4227027*X^2+5.84261
     89*X-12.97543343
1930 GOTO 1950
1940 P(3)=-.90010045*X^4+5.59944
     14*X^3-13.74668558*X^2+18.4
     861602*X-17.94291787
1950 X=V(4)
1955 H$="TWO"
1960 IF X>4.7 OR X<.4 THEN 5930
1970 IF X<1.644 THEN 2000
1980 P(2)=-.02886906*X^4+.433457
     3*X^3-2.56215996*X^2+8.5095
     607*X-15.77926023
1990 GOTO 3410
2000 P(2)=-.52545885*X^4+3.83185
     57*X^3-10.78317301*X^2+16.7
     8993426*X-18.64659637
3410 P(1)=10^(P(1)/10)
3450 P(2)=10^(P(2)/10)
3490 P(3)=10^(P(3)/10)
3530 R=10^(R/10)
3570 PRINT
3610 FOR I=1 TO 3
3650 S(I,1)=P(I)/(R*B(I))*Z^2-X(
     I)^2
```

```
3690 S(I,2)=P(I)/(R*B(I))*Z*COS(
     Z1)-X(I)*COS(P0(I))
3730 S(I,3)=X(I)*SIN(P0(I))-Z*(P
     (I)/(R*B(I)))*SIN(Z1)
3770 NEXT I
3810 FOR I=1 TO 3
3850 IF ABS(S(I,1))+ABS(S(I,2))+
     ABS(S(I,3))=0 THEN 5610
3890 NEXT I
3930 C(1,1)=S(2,2)*S(3,3)-S(3,2)
     *S(2,3)
3970 C(1,2)=-(S(2,1)*S(3,3)-S(3,
     1)*S(2,3))
4010 C(1,3)=S(2,1)*S(3,2)-S(3,1)
     *S(2,2)
4050 C(2,1)=-(S(3,3)*S(1,2)-S(3,
     2)*S(1,3))
4090 C(2,2)=S(3,3)*S(1,1)-S(3,1)
     *S(1,3)
4130 C(2,3)=-(S(3,2)*S(1,1)-S(3,
     1)*S(1,2))
4170 C(3,1)=S(2,3)*S(1,2)-S(2,2)
     *S(1,3)
4210 C(3,2)=-(S(2,3)*S(1,1)-S(2,
     1)*S(1,3))
4250 C(3,3)=S(2,2)*S(1,1)-S(2,1)
     *S(1,2)
4290 D=S(1,1)*C(1,1)+S(1,2)*C(1,
     2)+S(1,3)*C(1,3)
4330 IF D=0 THEN 5610
4370 FOR I=1 TO 3
4410 FOR J=1 TO 3
4450 H(I,J)=C(J,I)/D
4490 NEXT J
4530 NEXT I
4570 FOR I=1 TO 3
4610 G6(I)=H(I,1)*(1-P(1)/(R*B(1
     )))+H(I,2)*(1-P(2)/(R*B(2))
     )+H(I,3)*(1-P(3)/(R*B(3)))
4650 NEXT I
4670 DEG
4690 G7=ABS(G6(1))
4730 G7=SQR(G7)
4740 G8=G6(3)/G6(2)
4750 IF ABS(G8)>60 THEN 4810
4760 IF G6(2)<0 THEN 4790
4770 G9=ATN(G8)
4780 GOTO 5200
4790 G9=180+ATN(G8)
4800 GOTO 5200
4810 IF G6(3)<0 THEN 4840
4820 G9=90
4830 GOTO 5200
4840 G9=-90
5200 PRINT
5210 PRINT
5250 PRINT
5290 PRINT
5330 PRINT
5370 PRINT USING 5450 , G7
```

```
5380 PRINT
5390 PRINT USING 5410 ; G9
5410 IMAGE "ANGLE ",MDDD.DDD
5450 IMAGE "GAMMA MAGNITUDE ",DD
     D.DDDD
5460 PRINT
5462 PRINT
5570 GOTO 5690
5610 DISP "ERROR IN MATRIX MANIP
     ULATION"
5650 PRINT "ERROR IN MATRICE"
5690 BEEP
5730 WAIT 100
5770 BEEP
5810 CLEAR
5850 GOTO 1090
5890 CLEAR
5930 BEEP
5970 DISP "POWER LEVEL"
6010 DISP
6020 PRINT H$
6050 BEEP
6090 BEEP
6130 END
```

```
6CAL    40 DISP
        50 DISP "ENTER DATE&TRIAL #"
        60 INPUT R$,V7
        70 DISP
        80 PRINT USING 100 ; R$,V7
        90 PRINT
       100 IMAGE "6CAL" , 8X,6A,6X,DDDD
       110 PRINT "_____________________
           _________"
       120 PRINT
       130 PRINT
       150 INTEGER I,J
       160 DIM P1(3),P2(3),X(3),R(3,4)
       170 DIM A(2,2),B0(2),X0(3),P0(3)
       180 DIM V(4),P(3,6),E(6),B6(3)
       360 REM PARAMETERS OF FOUR
                 SHORTS
       365 RAD
       370 P2(0)=.5279*PI
       380 P2(1)=PI
       390 P2(2)=-.558*PI
       400 P2(3)=-.058*PI
       410 DISP "FREQ IN  MHz"
       420 INPUT E3
       430 CLEAR
       440 PRINT USING 450 ; E3
       450 IMAGE 20X,DDDD,2X,"MHz"
       451 FOR I=0 TO 3
       452 E4(I)=PI-P2(I)
       453 E6(I)=E4(I)*30/(4*PI)
       454 NEXT I
       455 E5=30000/E3
       456 FOR I=0 TO 3
       457 P2(I)=-4*PI*E6(I)/E5+PI
       458 NEXT I
       460 PRINT
       470 PRINT "FOUR SHORTS"
       480 PRINT "------------"
       490 FOR J=0 TO 3
       500 P0=P2(J)/PI
       510 PRINT USING 520 ; J,P0
       520 IMAGE "PHIL(",D,")= ",DDD.DD
           D,"*π",/
       530 NEXT J
       540 C=2
       550 WAIT 50
       560 OUTPUT 706 USING "#,K,K" ; "
           H",C,"AJ","F"
       570 S=0
       580 FOR J=1 TO 5
       590 WAIT 100
       600 ENTER 706 USING "#,W" ; V(2)
       610 S=S+V(2)
       620 NEXT J
```

```
630 S=S/5
640 S=S*(5/1022)
650 X=S
655 Q$="INITIAL"
660 IF X>4.98 OR X<1.3 THEN 4870
670 V8=-.01964561*X^4+.32342664*
    X^3-2.17641437*X^2+8.7196227
    9*X-14.11138973
680 CLEAR
690 DISP
700 DISP
710 DISP "POWER LEVEL"
720 DISP
730 DISP V8
740 INPUT Q$
750 IF Q$#"C" THEN 540
760 CLEAR
770 PRINT
780 PRINT
790 PRINT "INCIDENT POWER (dBm)"
800 PRINT "----------------------"
810 CLEAR 7
820 FOR L=1 TO 5
830 IF L#1 THEN 860
840 A$="USE MATCHED LOAD"
850 GOTO 960
860 IF L#2 THEN 890
870 A$="USE SHORT 0 "
880 GOTO 960
890 IF L#3 THEN 920
900 A$="USE SHORT 1"
910 GOTO 960
920 IF L#4 THEN 940
930 A$="USE SHORT 2"
940 IF L#5 THEN 960
950 A$="USE SHORT 3"
960 DISP A$
970 BEEP 40,100
980 DISP "READY (Y)?"
990 DISP
1000 INPUT Q$
1010 CLEAR
1020 CLEAR 7
1030 V(1)=0
1040 V(2)=0
1050 V(3)=0
1060 V(4)=0
1070 FOR I=1 TO 10
1080 OUTPUT 706 USING "#,K,K" ;
     "H",1,"AJ","F"
1090 WAIT 300
1100 ENTER 706 USING "#,W" ; S
1110 V(1)=V(1)+S/2044
1120 OUTPUT 706 USING "#,K,K" ;
     "H",2,"AJ","F"
1130 WAIT 300
1140 ENTER 706 USING "#,W" ; S
1150 V(2)=V(2)+S/2044
1160 OUTPUT 706 USING "#,K,K" ;
     "H",4,"AJ","F"
```

```
1170 WAIT 300
1180 ENTER 706 USING "#,W" ; S
1190 V(3)=V(3)+S/2044
1200 OUTPUT 706 USING "#,K,K" ;
     "H",8,"AJ","F"
1210 WAIT 300
1220 ENTER 706 USING "#,W" ; S
1230 V(4)=V(4)+S/2044
1240 NEXT I
1250 OUTPUT 706 USING "#,K" ; "H
     "
1260 X=V(1)
1265 O$="P1"
1270 IF X>4.9 OR X<.3 THEN 4870
1280 IF X<1.297 THEN 1310
1290 P(1,L)=-.01491633*X^4+.2409
     8242*X^3-1.57315175*X^2+6.0
     3689409*X-12.68435425
1300 GOTO 1320
1310 P(1,L)=-.32255049*X^4+4.843
     33171*X^3-13.99801255*X^2+1
     8.53171147*X-17.16251206
1320 X=V(2)
1325 O$="REF"
1330 IF X>4.98 OR X<1.3 THEN 487
     0
1340 E(L)=-.01964561*X^4+.323426
     64*X^3-2.17641437*X^2+8.719
     62279*X-14.11138973
1350 PRINT E(L)
1360 X=V(3)
1365 O$="P3"
1370 IF X>4.75 OR X<.561 THEN 48
     70
1380 IF X<1.8 THEN 1410
1390 P(3,L)=-.0120374*X^4+.20481
     734*X^3-1.4227027*X^2+5.842
     6189*X-12.97543343
1400 GOTO 1420
1410 P(3,L)=-.90010045*X^4+5.599
     4414*X^3-13.74668558*X^2+18
     .48613602*X-17.94291787
1420 X=V(4)
1425 O$="P2"
1430 IF X>4.7 OR X<.4 THEN 4870
1440 IF X<1.644 THEN 1470
1450 P(2,L)=-.02886906*X^4+.4334
     573*X^3-2.56215996*X^2+8.50
     95607*X-15.77926023
1460 GOTO 1480
1470 P(2,L)=-.5254585*X^4+3.831
     8557*X^3-10.78317301*X^2+16
     .78993426*X-18.64659637
1480 P(1,L)=10^(P(1,L)/10)
1490 P(2,L)=10^(P(2,L)/10)
1500 P(3,L)=10^(P(3,L)/10)
1510 E(L)=10^(E(L)/10)
1520 NEXT L
1530 FOR I=1 TO 3
1540 B6(I)=P(I,1)/E(1)
```

```
1550 R(I,0)=P(I,2)/(E(2)*B6(I))
1560 R(I,1)=P(I,3)/(E(3)*B6(I))
1570 R(I,2)=P(I,4)/(E(4)*B6(I))
1580 R(I,3)=P(I,5)/(E(5)*B6(I))
1590 NEXT I
1600 PRINT
1610 PRINT
1620 FOR J=0 TO 3
1630 FOR I=1 TO 3
1640 W3=J+1
1650 PRINT USING 1660 ; I,W3,R(I
     ,J)
1660 IMAGE "R(",D,D,")",2X,DD.DD
     D
1670 NEXT I
1680 PRINT
1690 NEXT J
1700 PRINT
1710 PRINT
1720 REM INITIAL GUESS
1730 REM GAMMA VECTOR - G1,G2,G3
1735 RAD
1740 DIM M(3,3),Z1(3),D(3)
1750 D=1
1760 M1=SIN(P2(2)-P2(3))+SIN(P2(
     3)-P2(1))+SIN(P2(1)-P2(2))
1770 S0=SIN(P2(0))
1780 S1=SIN(P2(1))
1790 S2=SIN(P2(2))
1800 S3=SIN(P2(3))
1810 C0=COS(P2(0))
1820 C1=COS(P2(1))
1830 C2=COS(P2(2))
1840 C3=COS(P2(3))
1850 G1=(SIN(P2(2)-P2(3))+SIN(P2
     (3)-P2(0))+SIN(P2(0)-P2(2))
     )/M1
1860 G2=(SIN(P2(3)-P2(1))+SIN(P2
     (1)-P2(0))+SIN(P2(0)-P2(3))
     )/M1
1870 G3=(SIN(P2(1)-P2(2))+SIN(P2
     (2)-P2(0))+SIN(P2(0)-P2(1))
     )/M1
1880 M(1,1)=R(1,0)-R(1,1)*G1-R(1
     ,2)*G2-R(1,3)*G3
1890 M(2,1)=R(2,0)-R(2,1)*G1-R(2
     ,2)*G2-R(2,3)*G3
1900 M(3,1)=R(3,0)-R(3,1)*G1-R(3
     ,2)*G2-R(3,3)*G3
1910 M(1,2)=2*(R(1,0)*C0-R(1,1)*
     C1*G1-R(1,2)*C2*G2-R(1,3)*C
     3*G3)
1920 M(2,2)=2*(R(2,0)*C0-R(2,1)*
     C1*G1-R(2,2)*C2*G2-R(2,3)*C
     3*G3)
1930 M(3,2)=2*(R(3,0)*C0-R(3,1)*
     C1*G1-R(3,2)*C2*G2-R(3,3)*C
     3*G3)
1940 M(1,3)=-2*(R(1,0)*S0-R(1,1)
     *S1*G1-R(1,2)*S2*G2-R(1,3)*
     S3*G3)
```

```
1950 M(2,3)=-2*(R(2,0)*S0-R(2,1)
     *S1*G1-R(2,2)*S2*G2-R(2,3)*
     S3*G3)
1960 M(3,3)=-2*(R(3,0)*S0-R(3,1)
     *S1*G1-R(3,2)*S2*G2-R(3,3)*
     S3*G3)
1970 A2=M(2,1)*M(1,2)-M(1,1)*M(2
     ,2)
1980 A3=M(1,1)*M(2,3)-M(1,3)*M(2
     ,1)
1990 IF ABS(A2)<.0000000001 THEN
      2000 ELSE 2020
2000 IF A3>0 THEN P0=0 ELSE P0=P
     I
2010 GOTO 2060
2020 IF ABS(A3)<.0000000001 THEN
      2030 ELSE 2050
2030 IF A2>0 THEN P0=PI/2 ELSE P
     0=-PI/2
2040 GOTO 2060
2050 P0=ATN(A2/A3)
2060 IF ABS(M(1,1))>.00000000001
      THEN 2100
2070 Z0=0
2080 IF M(1,2)*COS(P0)+M(1,3)*SI
     N(P0)<=0 THEN P0=P0 ELSE P0
     =P0+PI
2090 GOTO 2140
2100 A1=-(M(1,2)*COS(P0)+M(1,3)*
     SIN(P0))/M(1,1)
2110 IF A1>=2 THEN P0=P0 ELSE P0
     =P0+PI
2120 A1=-(M(1,2)*COS(P0)+M(1,3)*
     SIN(P0))/M(1,1)
2130 Z0=(A1-SQR(A1*A1-4))/2
2140 Z2=Z0*COS(P0)
2150 Z3=Z0*SIN(P0)
2160 GOTO 3160
2170 DIM C(3,4),S(3),T(3,4),Y(3)
2180 REM C(3,3) - COEFFICIENT MA
     TRIX, C(I,4) - RHS VECTOR,
     S(3) - SOLUTION VECTOR
2190 FOR I=1 TO 3
2200 FOR J=1 TO 3
2210 C(I,J)=M(I,J)
2220 NEXT J
2230 NEXT I
2240 FOR I=1 TO 3
2250 C(I,4)=D(I)
2260 NEXT I
2270 REM ENTER SUB SOLUTION OF A
      SET OF 3 LINEAR EQUATIONS
2280 GOSUB 2300
2290 GOTO 3160
2300 REM SUB SOLUTION OF 3 LINEA
     R EQUATIONS
2310 FOR I=1 TO 3
2320 FOR J=1 TO 4
2330 T(I,J)=C(I,J)
2340 NEXT J
```

```
2350 NEXT I
2360 D=1
2370 E=.000001 ! MINIMUM ALLOWAB
     LE MAGNITUDE FOR A PIVOT EL
     EMENT
2380 FOR K=1 TO 3
2390 K1=K-1
2400 P=0
2410 FOR I=1 TO 3
2420 FOR J=1 TO 3
2430 IF K=1 THEN 2500
2440 FOR I2=1 TO K1
2450 FOR J2=1 TO K1
2460 IF I=I(I2) THEN 2540
2470 IF J=J(J2) THEN 2540
2480 NEXT J2
2490 NEXT I2
2500 IF ABS(T(I,J))<=ABS(P) THEN
      2540
2510 P=T(I,J)
2520 I(K)=I
2530 J(K)=J
2540 NEXT J
2550 NEXT I
2560 IF ABS(P)>E THEN 2590
2570 D=0
2580 RETURN
2590 I3=I(K)
2600 J3=J(K)
2610 D=D*P
2620 FOR J=1 TO 4
2630 T(I3,J)=T(I3,J)/P
2640 NEXT J
2650 T(I3,J3)=1/P
2660 FOR I=1 TO 3
2670 T=T(I,J3)
2680 IF I=I3 THEN 2730
2690 T(I,J3)=-T/P
2700 FOR J=1 TO 4
2710 IF J<>J3 THEN T(I,J)=T(I,J)
     -T*T(I3,J)
2720 NEXT J
2730 NEXT I
2740 NEXT K
2750 FOR I=1 TO 3
2760 I4=I(I)
2770 J4=J(I)
2780 O1(I4)=J4
2790 S(J4)=T(I4,4)
2800 NEXT I
2810 T=0
2820 N1=2
2830 FOR I=1 TO N1
2840 P1=I+1
2850 FOR J=P1 TO 3
2860 IF O1(J)>=O1(I) THEN 2910
2870 T1=O1(J)
2880 O1(J)=O1(I)
2890 O1(I)=T1
2900 T=T+1
```

```
2910 NEXT J
2920 NEXT I
2930 IF INT(T/2)*2<>T THEN D=-D
2940 FOR J=1 TO 3
2950 FOR I=1 TO 3
2960 I4=I(I)
2970 J4=J(I)
2980 Y(J4)=T(I4,J)
2990 NEXT I
3000 FOR I=1 TO 3
3010 T(I,J)=Y(I)
3020 NEXT I
3030 NEXT J
3040 FOR I=1 TO 3
3050 FOR J=1 TO 3
3060 I4=I(J)
3070 J4=J(J)
3080 Y(I4)=T(I,J4)
3090 NEXT J
3100 FOR J=1 TO 3
3110 T(I,J)=Y(J)
3120 NEXT J
3130 NEXT I
3140 RETURN
3150 PRINT
3160 REM PRINT Z INITIAL GUESS
3170 REM CALCULATION OF Z USING
     LEAST SQUERS METHOD
3180 REM NONLINEAR EQUATIONS
3190 A4=M(1,1)^2+M(2,1)^2+M(3,1)
     ^2
3200 B4=M(1,1)*M(1,2)+M(2,1)*M(2
     ,2)+M(3,1)*M(3,2)
3210 C4=M(1,1)*M(1,3)+M(2,1)*M(2
     ,3)+M(3,1)*M(3,3)
3220 E4=M(1,2)^2+M(2,2)^2+M(3,2)
     ^2
3230 F4=-(M(1,1)^2+M(2,1)^2+M(3,
     1)^2)
3240 G4=M(1,2)*M(1,3)+M(2,2)*M(2
     ,3)+M(3,2)*M(3,3)
3250 H4=M(1,1)*M(1,2)+M(2,1)*M(2
     ,2)+M(3,1)*M(3,2)
3260 K4=M(1,3)^2+M(2,3)^2+M(3,3)
     ^2
3270 L4=M(1,1)*M(1,3)+M(2,1)*M(2
     ,3)+M(3,1)*M(3,3)
3280 REM INITIATE Y2 AND Y3
3290 Y2=Z2
3300 Y3=Z3
3310 REM TWO NONLINEAR EQUATIONS
3320 P2=2*A4*Y2^3+2*A4*Y2*Y3^2+3
     *B4*Y2^2+B4*Y3^2+2*C4*Y2*Y3
     +(E4-2*F4)*Y2+G4*Y3+H4
3330 P8=2*A4*Y3^3+2*A4*Y2^2*Y3+3
     *C4*Y3^2+C4*Y2^2+2*B4*Y2*Y3
     +(K4-2*F4)*Y3+G4*Y2+L4
3340 P4=6*A4*Y2^2+2*A4*Y3^2+6*B4
     *Y2+2*C4*Y3+E4-2*F4
3350 P5=6*A4*Y3^2+2*A4*Y2^2+6*C4
     *Y3+2*B4*Y2+K4-2*F4
```

```
3360 P6=4*A4*Y2*Y3+2*B4*Y3+2*C4*
     Y2+G4
3370 P7=4*A4*Y2*Y3+2*C4*Y2+2*B4*
     Y3+G4
3380 REM SOLUTION -NEWTON METHOD
3390 D4=P4*P5-P6*P7
3400 Z2=Y2-(P2*P5-P8*P6)/D4
3410 Z3=Y3-(P8*P4-P2*P7)/D4
3420 IF ABS(Y2-Z2)<.0000000001 A
     ND ABS(Y3-Z3)<.0000000001 T
     HEN 3460
3430 Y2=Z2
3440 Y3=Z3
3450 GOTO 3320
3460 Z0=SQR(Z2*Z2+Z3*Z3)
3470 X0(0)=Z0
3480 IF ABS(Z2)<.00000001 THEN 3
     510
3490 P0=ATN2(Z3,Z2)
3500 GOTO 3540
3510 IF Z3>.00000001 THEN P0=PI/
     2
3520 GOTO 3540
3530 IF Z3>-.00000001 THEN P0=0
     ELSE P0=-PI/2
3540 Q0=P0/PI
3550 P0(0)=P0
3560 REM
3570 P3=Q0*PI
3580 REM X(I), I=1,2,3 COMPUTATI
     ON - INITIAL GUESS
3590 DIM B(3,3),U(3)
3600 B(1,1)=1
3610 B(2,1)=1
3620 B(3,1)=1
3630 B(1,2)=2*C1
3640 B(2,2)=2*C2
3650 B(3,2)=2*C3
3660 B(1,3)=-2*S1
3670 B(2,3)=-2*S2
3680 B(3,3)=-2*S3
3690 FOR I9=1 TO 3
3700 REM RHS VECTOR
3710 U(1)=R(I9,1)*Z0*Z0+2*R(I9,1
     )*Z0*COS(P3)*C1-2*R(I9,1)*Z
     0*SIN(P3)*S1+R(I9,1)-1
3720 U(2)=R(I9,2)*Z0*Z0+2*R(I9,2
     )*Z0*COS(P3)*C2-2*R(I9,2)*Z
     0*SIN(P3)*S2+R(I9,2)-1
3730 U(3)=R(I9,3)*Z0*Z0+2*R(I9,3
     )*Z0*COS(P3)*C3-2*R(I9,3)*Z
     0*SIN(P3)*S3+R(I9,3)-1
3740 REM INITIAL GUESS COMPUTATI
     ON
3750 FOR I8=1 TO 3
3760 FOR J8=1 TO 3
3770 C(I8,J8)=B(I8,J8)
3780 NEXT J8
3790 NEXT I8
3800 FOR I8=1 TO 3
```

```
3810 C(I8,4)=U(I8)
3820 NEXT I8
3830 REM  CALL SUB SIM EQU
3840 GOSUB 2300
3850 IF ABS(D)>.000000000001 THE
     N 3890
3860 PRINT USING 3870 ; I9
3870 IMAGE "SET FOR X(",D,") HAS
      NO SOLUTION. PIVOT ELEMENT
      < 0.00001"
3880 GOTO 4390
3890 REM PRINT RESULTS
3900 X0(I9)=SQR(S(2)^2+S(3)^2)
3910 IF S(2)=0 THEN 3940
3920 P0(I9)=ATN2(S(3),S(2))
3930 GOTO 3960
3940 IF S(3)>0 THEN P0(I9)=PI/2
3950 IF S(3)=0 THEN P0(I9)=0 ELS
     E P0(I9)=-PI/2
3960 Q0=P0(I9)/PI
3970 REM TWO NONLINEAR EQUATIONS
      FOR X2 AND X3
3980 A5=C1+C2+C3
3990 B5=S1+S2+S3
4000 C5=C1*C1+C2*C2+C3*C3
4010 D5=R(I9,1)+R(I9,2)+R(I9,3)
4020 E5=R(I9,1)*C1+R(I9,2)*C2+R(
     I9,3)*C3
4030 F5=R(I9,1)*S1+R(I9,2)*S2+R(
     I9,3)*S3
4040 G5=S1*C1+S2*C2+S3*C3
4050 H5=R(I9,1)*C1*C1+R(I9,2)*C2
     *C2+R(I9,3)*C3*C3
4060 I5=R(I9,1)*S1*C1+R(I9,2)*S2
     *C2+R(I9,3)*S3*C3
4070 J5=S1*S1+S2*S2+S3*S3
4080 M5=R(I9,1)*S1*S1+R(I9,2)*S2
     *S2+R(I9,3)*S3*S3
4090 S6=SIN(P3)
4100 C6=COS(P3)
4110 REM INITIATE X2 AND X3
4120 X2=S(2)
4130 X3=S(3)
4140 REM START ITERATION
4150 L2=6*X2*X2*X2+6*X2*X3*X3+6*
     A5*X2*X2+2*A5*X3*X3-4*B5*X2
     *X3
4160 L2=L2+2*(2*C5-Z0*Z0*D5-2*Z0
     *C6*E5+2*Z0*S6*F5-D5+3)*X2-
     4*G5*X3
4170 L2=L2+2*(A5-E5-Z0*Z0*E5+2*Z
     0*S6*I5-2*Z0*C6*H5)
4180 L3=6*X3*X3*X3+6*X2*X2*X3-6*
     B5*X3*X3-2*B5*X2*X2+4*A5*X2
     *X3
4190 L3=L3+2*(2*J5-Z0*Z0*D5-2*Z0
     *C6*E5+2*Z0*S6*F5-D5+3)*X3-
     4*G5*X2
4200 L3=L3-2*(B5-F5-Z0*Z0*F5+2*Z
     0*S6*M5-2*Z0*C6*I5)
```

```
4210 L8=18*X2*X2+6*X3*X3+12*A5*X
     2-4*B5*X3+2*(2*C5-Z0*Z0*O5-
     2*Z0*C6*E5+2*Z0*S6*F5-O5+3)
4220 L5=12*X2*X3+4*A5*X3-4*B5*X2
     -4*G5
4230 L6=18*X3*X3+6*X2*X2-12*B5*X
     3+4*A5*X2+2*(2*J5-Z0*Z0*O5-
     2*Z0*C6*E5+2*Z0*S6*F5-O5+3)
4240 L7=12*X2*X3-4*B5*X2+4*A5*X3
     -4*G5
4250 D9=L8*L6-L5*L7
4260 V2=X2-(L2*L6-L3*L5)/D9
4270 V3=X3-(L3*L8-L2*L7)/D9
4280 IF ABS(V2-X2)<.0000000001 A
     ND ABS(V3-X3)<.0000000001 T
     HEN 4320
4290 X2=V2
4300 X3=V3
4310 GOTO 4150
4320 X0(I9)=SQR(V2*V2+V3*V3)
4330 IF V2=0 THEN 4360
4340 P0(I9)=ATN2(V3,V2)
4350 GOTO 4370
4360 IF V3>0 THEN P0(I9)=PI/2 EL
     SE P0(I9)=-PI/2
4370 Q0=P0(I9)/PI
4380 REM PRINT FINAL RESULTS
4390 NEXT I9
4400 REM PRINT FINAL RESULTS
4410 Q0=P0(0)/PI
4420 IMAGE "Z= ",M.DDDDE,/,"PHIZ
     = ",DDD.DDD,"*π"
4430 FOR I=1 TO 3
4440 Q0=P0(I)/PI
4450 IMAGE "X(",D,")= ",M.DDDDE,
     /,"PHIX(",D,")= ",DD.DDD,"*
     π"
4460 NEXT I
4470 IF O=1 THEN W1=.02 ELSE W1=
     .05
4480 Q9(1)=P0(0)
4490 Q9(2)=P0(1)
4500 Q9(3)=P0(2)
4510 Q9(4)=P0(3)
4520 Q8(1)=X0(0)
4530 Q8(2)=X0(1)
4540 Q8(3)=X0(2)
4550 Q8(4)=X0(3)
4560 ASSIGN# 1 TO "6DATA.WOODS"
4570 PRINT# 1 ; B6(1),B6(2),B6(3
     ),P0(0),P0(1),P0(2),P0(3),X
     0(0),X0(1),X0(2),X0(3)
4580 ASSIGN# 1 TO *
4590 PRINT
4600 PRINT
4610 PRINT
4620 PRINT "PHI'S"
4630 PRINT
4640 FOR I=0 TO 3
4650 PRINT P0(I)
```

```
4660 NEXT I
4670 PRINT
4680 PRINT "Z AND X'S"
4690 PRINT
4700 FOR I=0 TO 3
4710 PRINT X0(I)
4720 NEXT I
4730 PRINT
4740 PRINT "B'S"
4750 PRINT
4760 FOR I=1 TO 3
4770 PRINT B6(I)
4780 NEXT I
4790 PRINT
4800 PRINT
4810 PRINT
4820 PRINT
4830 PRINT "----------------------
     ------------"
4840 PRINT
4850 PRINT
4860 GOTO 4980
4870 BEEP
4880 BEEP
4890 WAIT 200
4900 BEEP
4910 CLEAR
4920 DISP X
4930 DISP
4940 DISP O$
4945 DISP
4950 DISP "READJUST POWER LEVEL"
4960 DISP
4965 INPUT Z$
4970 GOTO 540
4980 END
```

Appendix G

SIX PORT CONSTANTS FOUND BY GIRIMAJI [10]

Frequency (MHZ)	$z \angle \phi_z$	$X_1 \angle \phi_{x1}$	$X_2 \angle \phi_{x2}$	$X_3 \angle \phi_{x3}$	$\lvert B_1 \rvert$	$\lvert B_2 \rvert$	$\lvert B_3 \rvert$
900	$0.276 \angle 176^\circ$	$0.700 \angle 139.5^\circ$	$0.673 \angle 203.0^\circ$	$0.309 \angle 34.5^\circ$	0.248	0.305	0.230
920	$0.229 \angle 173^\circ$	$0.630 \angle 130.0^\circ$	$0.649 \angle 173.4^\circ$	$0.309 \angle 13.1^\circ$	0.255	0.293	0.234
940	$0.170 \angle 166^\circ$	$0.589 \angle 116.3^\circ$	$0.605 \angle 198.6^\circ$	$0.340 \angle -11.3^\circ$	0.259	0.279	0.235
960	$0.121 \angle 167^\circ$	$0.533 \angle 104.4^\circ$	$0.589 \angle 198.6^\circ$	$0.369 \angle -30.2^\circ$	0.261	0.264	0.238
980	$0.070 \angle 176^\circ$	$0.477 \angle 90.5^\circ$	$0.567 \angle 1970^\circ$	$0.408 \angle -47.0^\circ$	0.269	0.248	0.243
1000	$0.049 \angle 269^\circ$	$0.410 \angle 69.0^\circ$	$0.510 \angle 197.7^\circ$	$0.483 \angle -58.1^\circ$	0.272	0.231	0.250
1020	$0.098 \angle -69^\circ$	$0.392 \angle 51.0^\circ$	$0.500 \angle 198.0^\circ$	$0.506 \angle -66.7^\circ$	0.270	0.213	0.254
1040	$0.150 \angle -65^\circ$	$0.395 \angle 32.7^\circ$	$0.483 \angle 197.8^\circ$	$0.522 \angle -74.0^\circ$	0.266	0.194	0.254
1060	$0.195 \angle -66^\circ$	$0.406 \angle 16.5^\circ$	$0.472 \angle 197.5^\circ$	$0.523 \angle -80.1^\circ$	0.268	0.178	0.259
1080	$0.232 \angle -70^\circ$	$0.421 \angle 13.6^\circ$	$0.475 \angle 197.6^\circ$	$0.523 \angle -86.7^\circ$	0.265	0.162	0.260
1100	$0.257 \angle -75^\circ$	$0.436 \angle -9.0^\circ$	$0.472 \angle 183.0^\circ$	$0.513 \angle -93.0^\circ$	0.260	0.147	0.259

Appendix H

RETURN LOSS AND INSERTION LOSS FOUND BY GIRIMAJI [10]

Insertion loss between ports 1-3, 1-4, 2-5, 2-4 and 3-5 of the five-port junction.

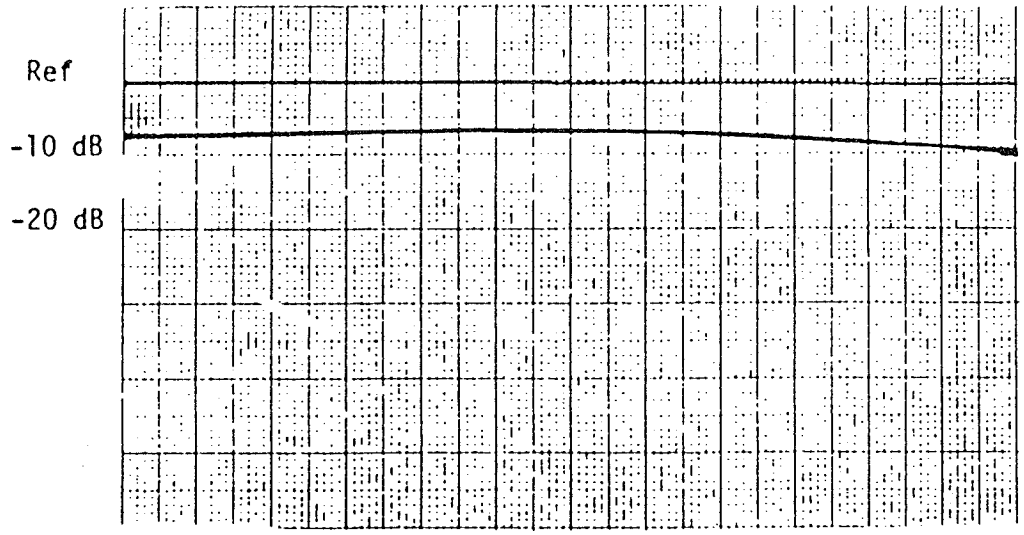

Insertion loss between ports 2-3, 4-3, 4-5, 1-5 and 1-2 of the five-port junction.

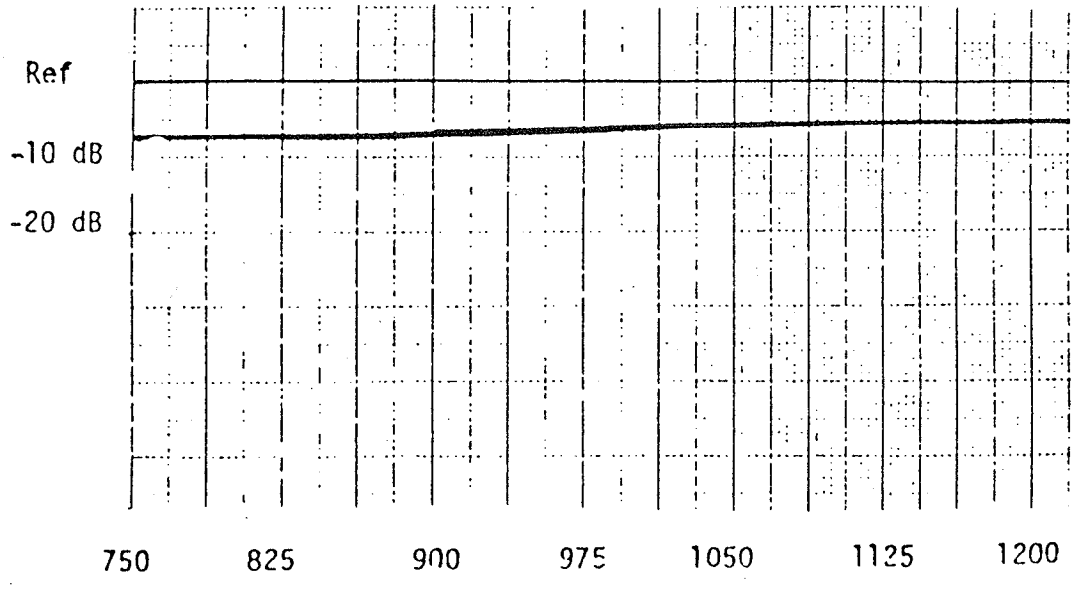

Appendix H

RETURN LOSS AND INSERTION LOSS FOUND BY GIRIMAJI [10]

Return Loss measurements for ports 1,2,3,4 and 5 of the five-port junction.